

UNCLASSIFIED

AD 296 180

*Reproduced
by the*

**ARMED SERVICES TECHNICAL INFORMATION AGENCY
ARLINGTON HALL STATION
ARLINGTON 12, VIRGINIA**



UNCLASSIFIED

NOTICE: When government or other drawings, specifications or other data are used for any purpose other than in connection with a definitely related government procurement operation, the U. S. Government thereby incurs no responsibility, nor any obligation whatsoever; and the fact that the Government may have formulated, furnished, or in any way supplied the said drawings, specifications, or other data is not to be regarded by implication or otherwise as in any manner licensing the holder or any other person or corporation, or conveying any rights or permission to manufacture, use or sell any patented invention that may in any way be related thereto.

63-2-4

HEL-2-2

CATALOGED BY ASTIA
AS AD NO. 296180

296180

INVESTIGATION ON A TWO-PHASE PROBLEM IN CLOSED PIPES

by

Walter Hans Graf



HYDRAULIC ENGINEERING LABORATORY
WAVE RESEARCH PROJECTS

UNIVERSITY OF CALIFORNIA
BERKELEY

University of California
Hydraulic Engineering Laboratory
Wave Research Projects

Submitted under Contract DA-49-055-CIV-ENG-63-4 with the
Beach Erosion Board, Corps of Engineers, U. S. Army

Institute of Engineering Research
Technical Report
HEL - 2 - 2

INVESTIGATION ON A TWO-PHASE
PROBLEM IN CLOSED PIPES

by

Walter Hans Graf

Berkeley, California
December, 1962

TABLE OF CONTENTS

| | Page |
|---|-------------|
| I Abstract | ii |
| II Introduction | 1 |
| III The Experimental Apparatus | 3 |
| IV The Loop System | 14 |
| V The Venturi Meter | 38 |
| VI Summary, Conclusions and Suggestions for Future Studies | 66 |
| VII Acknowledgement | 68 |
| VIII Nomenclature | 69 |
| IX References | 72 |
| X Appendix | 73 |

AUTHOR'S SUGGESTED SUBJECT INDEX

1. Micromeritics, (according to subject list of "Applied Mechanics Review")
 - (a) Dynamics of small particles
 - (b) Transport of particles by liquids
 - (c) Experimental techniques and measurement
2. Hydraulics (according to subject list of "Applied Mechanics Review")
Experimental techniques and measurement
3. Sediment Transport in Pipes
4. Two-phase Flow
5. Hydrocyclone
6. Venturimeter (modified 2-phase flow)
7. Measuring Concentration

INVESTIGATION ON A TWO-PHASE PROBLEM IN CLOSED PIPES

by

Walter Hans Graf

I. ABSTRACT

This investigation is a contribution to our knowledge of the two-phase flow problem. Two measuring devices for water-sand mixtures were tested, a Loop system and a special Venturi meter. The Loop system consisted of two identical vertical pipe sections with opposite flow direction. Head loss readings were obtained at both pipes. The summation of the readings could be correlated with the flow rate and their difference appeared to be proportional to the sediment concentration. The experimental results were obtained in a piece of equipment, especially developed for the study of water-solids mixtures in pipes. In the second part a Venturi meter was investigated. The Venturi meter was put in the system in a horizontal position. The pressure drop and the energy loss were observed. The drop was plotted versus the flow rate and a modified loss correlated with the sediment concentration. An attempt was made to explain the results theoretically. It is necessary hereby to describe the resistance of the grains in water for accelerated and decelerated motion.

II. INTRODUCTION

The scope of this report was to develop a device which would measure the flow rate and concentrations in a solid-liquid mixture. This is a two-phase problem, with water as the liquid phase and sand as the solid phase.

In the case of the one-phase flow problem a sudden change in head, caused by a change in cross section, can be calibrated to indicate the flowrate in the system. Application of this phenomenon is made in the different flowmeters, like the Venturi meter, the orifice meter, etc.

A Venturi meter was tested for its applicability in a two-phase system. The head drop should give us some information about the flowrate and it was hoped that another measurement on the same instrument such as the head loss across the Venturi meter might give us some information about the sediment concentration. This Venturi meter application is discussed in Chapter V of this report.

In addition to the Venturi meter another system was believed to give the desired information namely, flow rate and sediment concentration. This system is called a "Loop" system. The Loop system consists of two vertical pipes of equal length and of opposite flow direction. Head readings are obtained across each of the vertical pipes. If the pipe length is the same in both sections, a summation of the head loss in both vertical pipes will give us information about the flow rate. The concentration might be found by obtaining the difference of the two head loss values. This should be equal to the static pressure of the submerged

weight of the solid phase over the length of both vertical pipe sections .

The Loop system is discussed in Chapter IV.

III. EXPERIMENTAL APPARATUS

A new piece of experimental equipment completely selfcontained and independent from other equipment in the Hydraulics Laboratory was constructed. This was necessary for following reason: (a) all pumps would be damaged by pumping solid material, (b) the entire water supply would become contaminated with sediment, and (c) the system would need more maintainance, since it would require frequent cleaning.

This system consisted of a centrifugal drive-pump, a driveline, a jet pump for the sand-water mixture, a dischargeline, a weighing device, a hydrocyclone or sand separator, and a return channel. Each component is discussed in more detail below. The entire system is shown in Fig. III-1 and Fig. III-2. Fig. III-1 is a general photograph of the equipment and Fig. III-2 is a schematic drawing of the equipment.

Drive Pump. The drive-pump was located one floor below the apparatus. This was necessary to facilitate priming this pump. Water was supplied from the return-channel and then pumped into the driveline. The pump was driven by a 20 HP 440V 3 phase motor and developed a capacity of 250 gpm at a head of 180 feet. The pump remained in good condition at the end of the experiments, indicating an efficient separation of drive-water and sand by the hydrocyclone.

Drive Line. The driveline leading from the discharge side of the drive-pump with a nominal diameter of 2 inches. A gatevalve was installed in this line and was used to regulate the discharge from the jet pump. This valve was completely open for maximum velocity in the discharge line.



H9009P

FIGURE III - I - EXPERIMENTAL EQUIPMENT

Driveline Sediment-line Loop System
 Valve Hydrocyclone Manometers
 Venturi
 Switches for Manometers Weighing Device
 Centrifugal Pump Return Channel

- List of Symbols
- B - Basket with Screen
 - BA - Balance
 - D - Drive line
 - DI - Discharge line
 - DO - Downcomer Section
 - RE - Return Channel
 - R - Riser Section
 - S - Separator
 - T - Pump
 - V - 3 way Valve
 - VM - Venturi Meter
 - W_{1,2,3} - Weir, 1, 2, 3
 - Z - Returnpipe
 - TV - Turnvalve
 - W - Weighing Tank

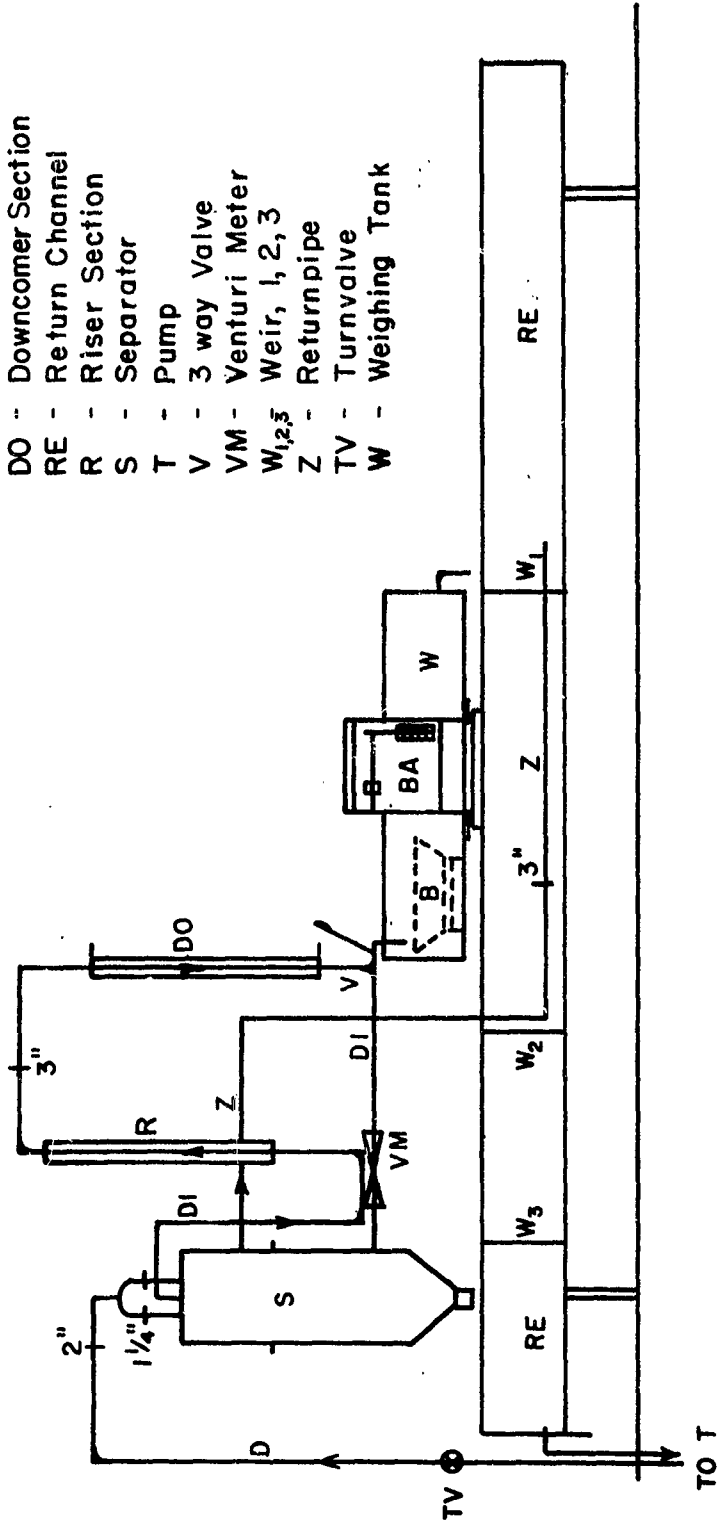


FIGURE III-2 - SCHEMATIC OF THE EXPERIMENTAL EQUIPMENT

H9012A

The jet pump was provided with two supply lines of 1-1/4 inch each. Therefore, the 2 inch drive line was divided into two 1-1/4 inch drive-lines near the jet pump.

Jetpump. The jetpump was developed in a previous study for pumping sand-water mixtures. The main flow of sand and water passed in the pump through a straight 2 inch pipe to reduce wear. Three jets entered this pipe at an angle of approximately 10° from the outside making the main pipe the mixing chamber. This chamber was followed by a diffuser which increased the main pipe to a 3 inch diameter. By increasing or decreasing the pressure in the jets, one is able to regulate the main flow.

The nozzle ring failed once, due to wear near the nozzles. A second nozzle ring lasted until the end of the experiment. The jetpump is described in Ref. 1.

Discharge Line. A 3 inch discharge line leaving the diffuser extended to the hydrocyclone. A number of elbows were necessary to obtain the desired alignment of the main pipe line. The discharge line contained the experimental units which were studied under two-phase flow.

Sampling Device. A 3-way valve was installed in the discharge line and permitted the flow to be interrupted and to be diverted into a sampling device. The sampling valve was designed from a standard pipe - T and a plunger, with rubber disks sealing against pipe surfaces. The rubber disks had to be replaced twice. Attached to the plunger was a micro-switch which was connected to a timer with 1/10 of a second least count. The sampling discharge was diverted into a weighing tank (94" x 34" x 20").

The mixture passed through a box with a screen bottom where the sand accumulated. After the weight of the mixture was obtained, the water was drained into the returnchannel and then the accumulated wet sand was weighed.

Hydrocyclon or Separation Tank. The hydrocyclon or separation tank making use of centrifugal force separated the solid phase from the liquid phase. Since the flow in such a device is rather complicated a small model was first constructed. After a number of trials, a satisfactory design was believed to be found. The model (Fig. III-3) was operated by a positive displacement pump, a sand-water mixture supply and an emergency jug, to catch the sand passing the cyclone. The model of the hydrocyclone, shown in Fig. III-4 and Fig. III-5 was made of lucite with a diameter of 5 inches, with the intake pipe at 2 inches above the bottom and the outlet about 5-1/2 inches above the bottom. A metal cone, with a diameter of 3-1/2 inches was then put into the model, with its highest point 2-1/2 inches above the bottom. Beneath the hood was ample space for sediment accumulation. At an elevation of 4-1/2 inches a baffle ring was installed. This ring was 1/2 inch wide. The wall of the container was kept dirty, for increasing the wall friction. The supply bottle was filled with sand and water. By means of adjusting the pipe relative to the sediment the concentration could be regulated. The tests gave the following results. The critical sand size with no accumulation was observed to be $d = 0.32$ mm. The test was started with a sand of size $d = 1.0$ mm. The discharge at the positive displacement pump was kept constant, to give a liquid velocity of $v_L = 1.77$ m/sec.

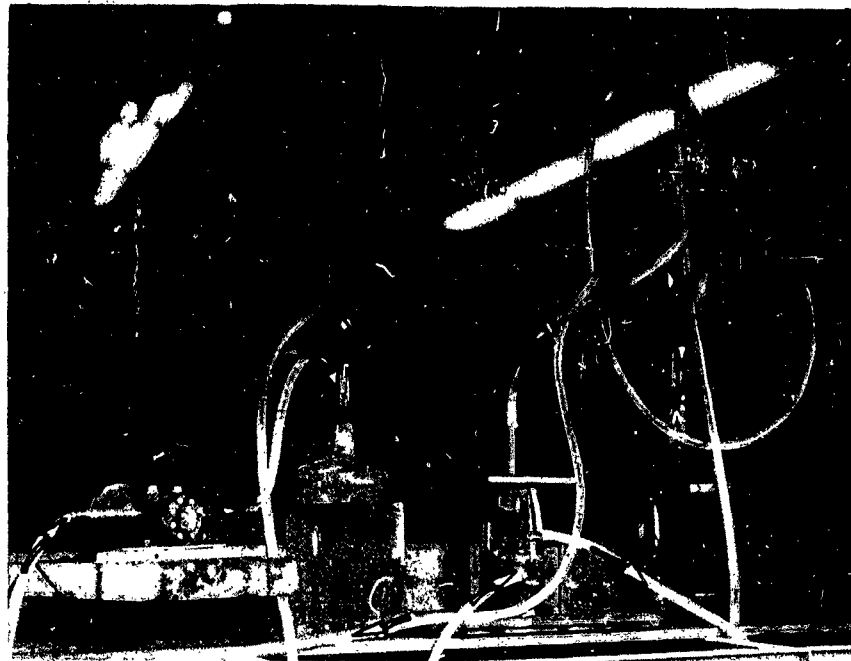
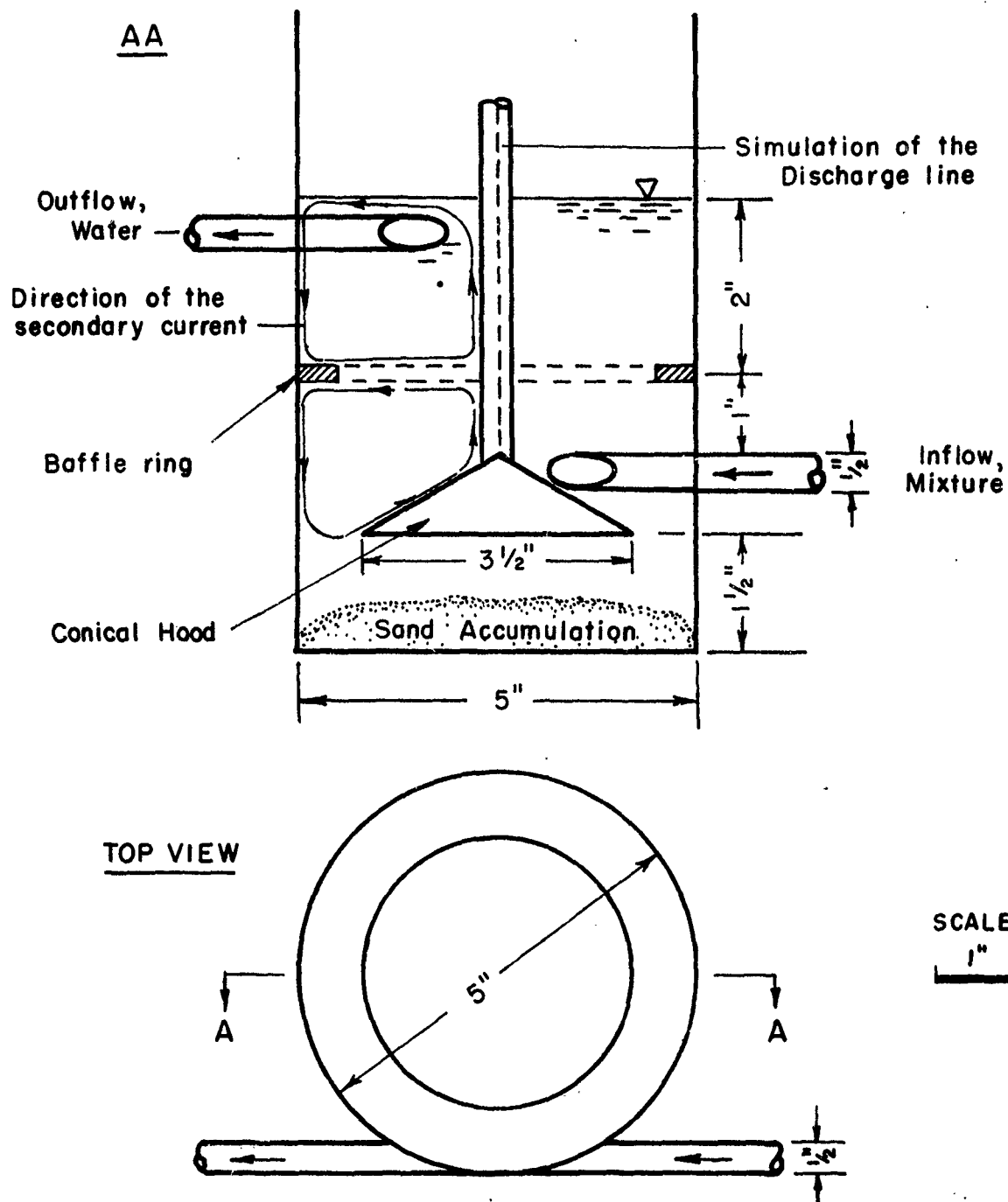


FIGURE III-3 - MODEL EQUIPMENT
Pump and Motor Supply Bottle Model Hydrocyclone Emergency Jug



FIGURE III-4 - MODEL OF HYDROCYCLONE

H9010P

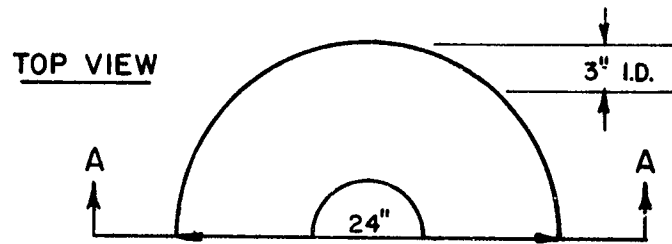
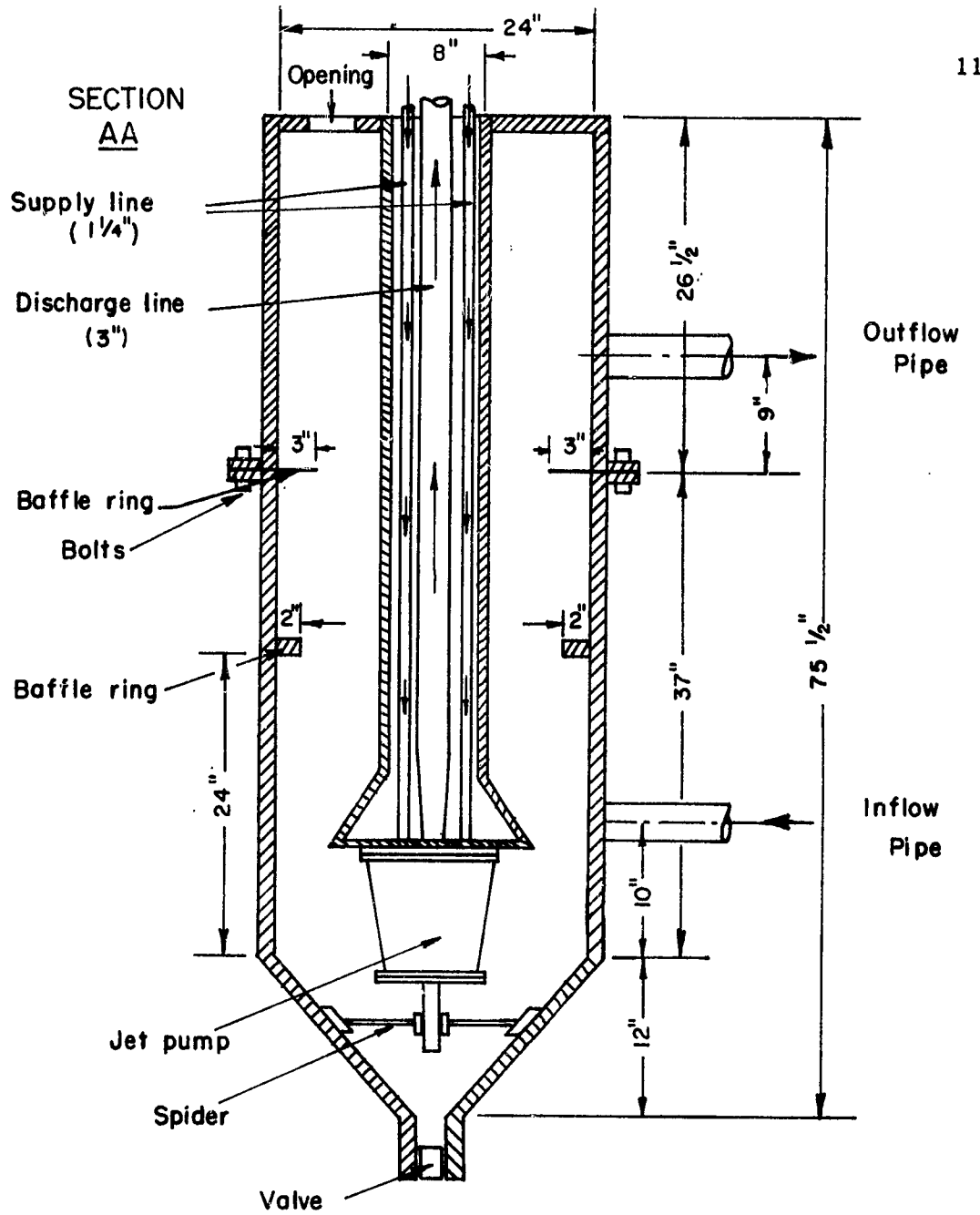


H9012A

FIGURE III-5 - MODEL OF SEPARATION TANK

Assuming that Froude's law governs this problem, i.e., that viscosity forces are of minor influence only, and taking the velocity $v_L = 1.77$ m/sec. and a grain diameter of $d = 3.2 \times 10^{-4}$ the Froude number v_L^2/gd equals 980. With a grain diameter of $d = 1.2 \times 10^{-3}$ we obtain from a Froude number of 980 a velocity of $v_L = 3.43$ m/sec. Therefore, the velocity where the given sand grain will be deposited in the hopper of the separation tank should be smaller than 3.43 m/sec. This value is slightly smaller than the maximum velocity used in the prototype, which is $v_{max} = 3.74$ m/sec. The operation of the prototype proved satisfactory. The intake pipe was installed so that the flow entered tangentially. The jet circled the tank and then the water rose. This rising motion continued until it reached the tangential outflow opening at the top of the separation tank. The inner and outer wall of the hydrocyclone should be of rough texture to increase friction and so cause the sand to settle. The sand has a chance to accumulate in the hopper on the bottom of the hydrocyclone. The motion of the water might be explained as a secondary current. An additional baffle ring was installed in the hydrocyclone to increase the separation efficiency.

The prototype was constructed as shown in Fig. III-6. It consisted of two parts such that the upper section could be lifted from the lower section. To the upper part an 8 inch pipe was welded, which contained the two drivepipes and the discharge pipe. The diameter of the cyclon was 2 feet and the total height was 75 1/2 inches. An opening on the top of the hydrocyclone permitted solids to be added and the valve



Scale
6"

H9013 A

FIGURE III-6 - SEPARATION TANK

on the bottom of the hopper permitted the system to be drained. The sediment collects in this hopper. The vertical distance between the intake and the outlet pipe is 26 inches. The inner wall of the hydrocyclone was extremely rough as formed by two baffle rings. During operation the hydrocyclone was open to the atmosphere and a parabolic water-surface at a height of the outlet pipe was observed. From the outlet pipe the water flows into the return channel.

Return Channel. The return channel, 3 feet wide and 30 feet long, was subdivided into 4 unequal settling basins. The first one was the longest and the last the shortest. Thus only the very finest particles of the dust sizes which have no abrasion effect reached the centrifugal pump. The efficiency of this settling basin therefore was satisfactory; however, the whole system, as well as the return channel, has to be cleaned after 40 hours of operation.

Manometer and Pressure Taps. Standard air-water manometers were used to measure differential heads. The pressure taps in the flow lines were made as follows: A 1/16 inch hole was drilled through the pipe. A standard 1/8 inch coupling then was welded on the outside of the pipe. A 1/16 inch hole was sufficient to prevent solids from entering the manometer. The connecting line from the pressure taps to the manometer was saran tubing.

Water. The water used was taken from the general water-supply system in the Hydraulics Laboratory. At the beginning the water was clean and clear. After operation with sand, the water became increasingly turbid;

therefore, it was necessary to clean the entire system frequently. The water temperature was recorded and found to vary from 78°F to 85°F during the entire series of the experiment.

IV. THE LOOP SYSTEM

The Loop System consists essentially of two identical vertical pipe sections with opposite flow directions. The head differences were obtained over the vertical pipe sections. It was expected that the summation of the head differences would determine the flow rate while their difference would determine the specific weight and, therefore, the concentration of two-phase flow in the vertical pipes. The experimental verification of the theory is presented below.

1. Theoretical Considerations

The different hydraulic equations for the liquid phase ^{are} derived in the conventional manner as follows, and the effect of the solid phase is then considered as an external force.

1.1. Basic Equations.

First the equation will be set up in a very general way, and then we shall consider them in an application for the Loop system.

1.1.1. Continuity Equation. The continuity equation states that the average velocity over a cross section multiplied by the area of the cross section is a constant. This constant is equal to the flow rate in volume per unit time.

(a) First this equation is applied to the solid phase. The fraction of area which is occupied by the solid phase is written as A_c . The velocity of the solid phase may be designated as v_s and the flow rate may be denoted as Q_s . And so the continuity equation reads:

$$Q_s = A_c \cdot v_s = \text{const.} \quad (1)$$

(b) If $A \cdot (1-c)$ represents the area of the liquid phase, v_L its velocity, and Q_L its flowrate, then the continuity equation for the liquid phase is:

$$Q_L = A \cdot (1-c) \cdot v_L = \text{const.} \quad (2)$$

(c) Also the total flow rate of both phases will obey the law of continuity. That is:

$$Q_S + Q_L = Q = \text{const.} \quad (3)$$

Furthermore, we shall establish a ratio of solid flow rate to total flow rate and shall call this ratio α .

$$Q_S / Q = \alpha \quad (4)$$

or rewriting equation (4):

$$(Q_S + Q_L) \alpha = Q \alpha = Q_S \quad (41)$$

The same stated for the ratio of liquid flow rate to total flow rate

$$Q_L / Q = (1 - \alpha) \quad (5)$$

and $(Q_S + Q_L)(1 - \alpha) = Q(1 - \alpha) = Q_L \quad (51)$

Q_S and Q_L in equation (4) and equation (5) can be replaced by equation (1) and

(2). Such combinations result in the following relationships.

$$Q_S = c \cdot A \cdot v_S = Q \cdot \alpha \quad (6)$$

and $Q_L = (1-c) \cdot A \cdot v_L = Q \cdot (1-\alpha) \quad (7)$

We may say that equation (3) could be written as

$$Q = v \cdot A \quad (3)$$

Where A is the total area of the pipe and v is an average velocity over

the cross section A. Combining now equation (3) and equation (6) amounts to:

$$v = \frac{Q}{A} = \frac{c}{\alpha} \bar{v}_s \quad (8)$$

and a combination of equation (3) with equation (7) gives us:

$$V = \frac{Q}{A} = \frac{(1-c)}{(1-\alpha)} \bar{v}_L \quad (9)$$

For all practical purposes in the Loop system one may assume that $\bar{v}_s \cong \bar{v}_L = v$ and therefore c may be written also in place of α . Also, this assumption will imply uniform concentration c in the entire Loop system.

1.12. Momentum Equation. Newton's second law of motion states: The time rate of change of the linear momentum of a body is directly proportional to the force acting on the body. Suppose m is the mass of the particle, v the instantaneous linear velocity and ΣF is the sum of all external forces acting on the particle, this equation may be written as:

$$\Sigma F = \frac{d}{dt} (m \cdot v) \quad (10)$$

Since $(m \cdot v)$ is a momentum, this equation is also referred to as the momentum equation. Assuming there is no change of mass with respect to time, one may write:

$$\Sigma F = m \frac{dv}{dt} \quad (11)$$

The problem to be investigated is a steady flow problem, so that

$$\frac{dv}{dt} = \frac{\partial v}{\partial t} + v \frac{\partial v}{\partial s} = \frac{dv}{ds} \quad (12)$$

Using the result of equation (12) and substituting it into equation

(11) we obtain:

$$\Sigma F = m \cdot \left(v \frac{dv}{ds} \right) \quad (13)$$

The application of this equation to pipe system shall now be investigated on hand of Fig. IV-1.

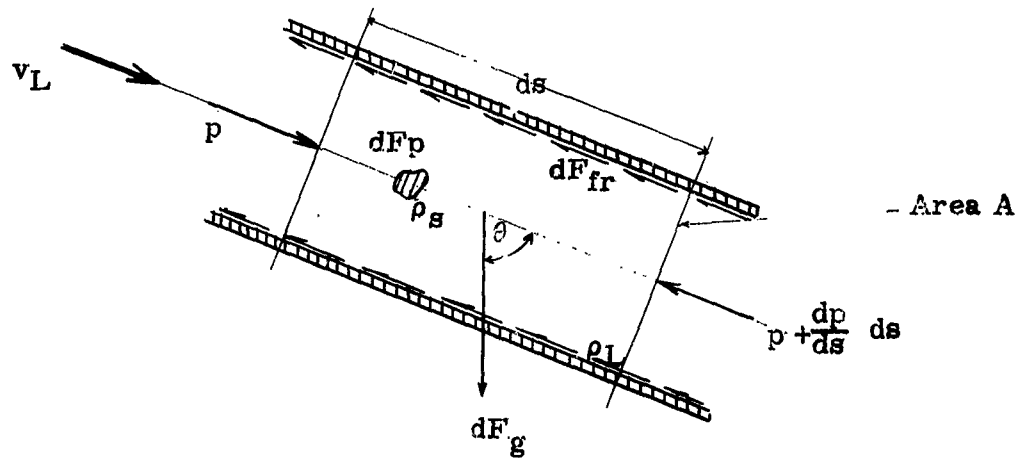


Fig. IV-1

A control volume element is considered over the length ds . The cross sectional area will be denoted with A . The liquid shall have the density ρ_L and g will be the acceleration due to gravity. The mass of the liquid involved is $\rho_L \cdot A \cdot ds \cdot (1-c)$. The acceleration according to equation (12) is $v_L \frac{dv_L}{ds}$. A pressure force of $p \cdot A \cdot (1-c)$ acts at the entrance and a pressure force in the opposite direction of $(p + \frac{dp}{ds} ds) \cdot A \cdot (1-c)$ acts at the exit. The gravitational force of $\rho_L \cdot A \cdot ds \cdot (1-c) \cdot g \cdot \cos \theta$ acts in the direction of ds . The frictional forces

dF_{fr} will oppose the flow. The particle in the flow may not have the same velocity as the liquid. They will then exert a force on the flow which may be positive if it retards the flow. It may be designated as dF_p . We shall now enter these terms into equation (11). So that we have:

$$\left[\rho_s \cdot ds \cdot A \cdot (1-c) \right] \cdot v_L \frac{dv_L}{ds} = p \cdot A \cdot (1-c) - \left[p + \frac{dp}{ds} ds \right] \cdot A \cdot (1-c) + \rho_L \cdot g \cdot A \cdot ds \cdot (1-c) \cos \theta - dF_{fr} - dF_p \quad (14)$$

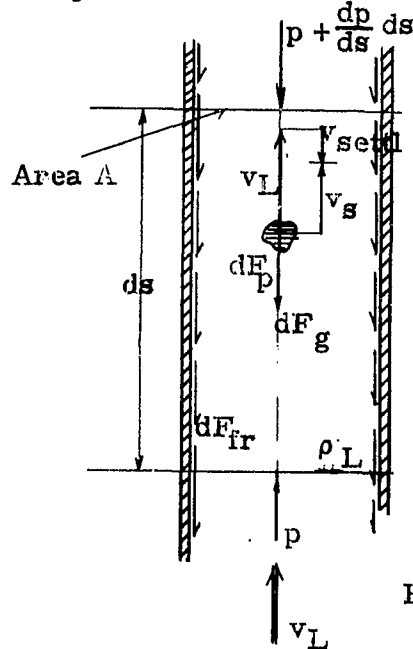
The equation is an extended dynamic equation with friction. Extended by the term dF_p . This is an external force, which is caused by the suspended particles in the flow. Such a force dF_p is the simplest way by which the effect of the solid phase may be expressed.

1.2 Application of the Momentum Equation to the "LOOP" System

1.21 Upward Flow Section or Riser Section. Equation (14) shall

be applied to the riser section. According to Fig. IV-2 the following signs will be obtained for the various terms assuming constant concentration.

Equation (14) now reads :



$$0 = (-dp \cdot A - \rho_L ds \cdot A \cdot g) \cdot (1-c) - dF_{fr} - dF_p \quad (15)$$

These forces are the net pressure force, the gravity force, the frictional force at the pipe wall and the particle force. The change in velocity dv , due to friction and particles shall be small, so that the left side of equation (14) becomes zero. All forces in equation

Fig. IV-2

(15) show a negative sign, that is to say they are opposing the flow.

Integration of equation (15) gives

$$0 = (-\Delta p \cdot A - \rho_L \cdot L \cdot A \cdot g) \cdot (1-c) - F_{fr} - F_p \quad (16)$$

Here L is the length of riser section. Considering F_p which represents the weight of the particles under water this gives:

$$F_p = A \cdot L \cdot c \cdot (\gamma_s - \gamma_L) \quad (17)$$

Using equation (17) and substituting it in equation (16) we obtain

$$0 = (-\Delta p \cdot A - \rho_L \cdot A \cdot g) \cdot (1-c) - (\rho_s - \rho_L) g \cdot A \cdot L \cdot c - F_{fr} \quad (18)$$

This equation was derived for a condition of upward flow. This section of the Loop system is called the riser section. The other part of the system, the downward flow section or downcomer section, is next discussed.

1.22 Downward Flow Section or Downcomer Section.

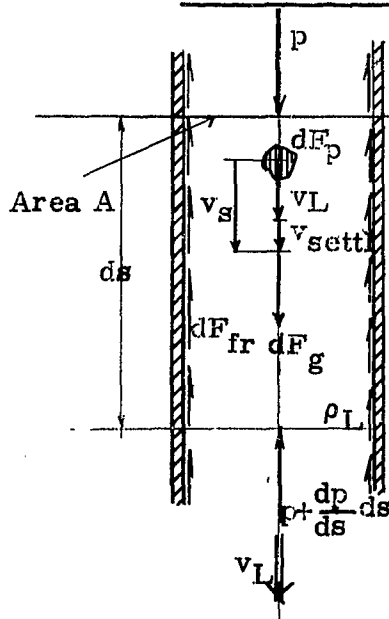


Fig. IV-3

Everything said in the previous part 1.21 applies here also, except that the sign of some of some of the forces will change, which can be seen in Fig. IV.3. Thus, equation (18) now reads:

$$0 = (-\Delta p + \rho_L L \cdot A \cdot g)(1-c) + (\rho_s - \rho_L) L \cdot A \cdot g \cdot c - F_{fr} \quad (19)$$

1.23 Summary of the Important Equations and a Logical Design of an Experiment . The most important equations of the previous chapters are equation (18) and equation (19) which for the riser section is

$$F_{fr} = (-\Delta p A - \rho_L \cdot L \cdot A \cdot g)(1-c) + (\rho_s - \rho_L) L \cdot A \cdot g \cdot c \quad (18)$$

for downcomer section is

$$F_{fr} = (-\Delta p A + \rho_L L \cdot A \cdot g)(1-c) + (\rho_s - \rho_L) L \cdot A \cdot g \cdot c \quad (19)$$

Dividing both equations by $A \cdot \gamma_L$ and we obtain for the riser section:

$$\frac{F_{fr}}{A \cdot \gamma_L} = \left(-\frac{\Delta p}{\gamma_L} - L \right) (1-c) - c \frac{\gamma_s - \gamma_L}{\gamma_L} L \quad (20)$$

for the downcomer section

$$\frac{F_{fr}}{A \cdot \gamma_L} = \left(-\frac{\Delta p}{\gamma_L} + L \right) (1 - c) + c \frac{\gamma_s - \gamma_L}{\gamma_L} L \quad (21)$$

The riser and downcomer sections are equal in geometry and flow conditions . Corresponding terms in equation (20) and equation (21) are thus of equal value . The influence of the various terms can thus be separated by mere addition or subtraction of the two equations . As shall be shown numerically , (this chapter part 3.3) the concentrations in equation (20) and equation (21) for our purpose are assumed to be the same . The first term in equation (20) and equation (21) may be recognized as a head across the length L . This head difference will be obtained across the two vertical sections at the Loop system .

1.24 Head Differences . We shall first write down the equation for the head difference in a vertical section . Regardless whether the flow goes upward or downward the head loss is due to the pipe roughness .

We may write:

$$\frac{\Delta p}{\gamma_L} + L = R \quad (22)$$

where R stands for reading on a manometer. For our purpose equation (22) is not sufficient, since it does not consider the suspended solids. We can, however, modify equation (22) such that we consider the pressure difference due to the solid phase. This effect of the suspended solids act with a positive sign in the riser section and with a negative sign in the downcomer section. Therefore, the modified equation (22) is

(a) for the riser section:

$$\left(-\frac{\Delta p}{\gamma_L} - L\right)(1-c) - L \left(\frac{\gamma_s - \gamma_L}{\gamma_L}\right) c = R_R \quad (23)$$

(b) for downcomer section:

$$\left(-\frac{\Delta p}{\gamma_L} + L\right)(1-c) + L \left(\frac{\gamma_s - \gamma_L}{\gamma_L}\right) c = R_D \quad (24)$$

The term $\left(-\frac{\Delta p}{\gamma} \pm L\right)(1-c)$ considers the frictional effect and its magnitude is the same in both sections and is termed R_{fr} . The other term $L \left(\frac{\gamma_s - \gamma_L}{\gamma_L}\right) c$ is due the suspended solids and is termed R_{susp} . So equation (28) and equation (29) can be written as

(a) for the riser section:

$$R_{fr} + R_{susp} = R_R \quad (25)$$

(b) for the downcomer section:

$$R_{fr} - R_{susp} = R_D \quad (26)$$

These head differences are then substituted into equation (20) and equation (21) and we get for the riser:

$$\frac{F_{fr}}{A \cdot \gamma_L} = R_R = R_{fr} + R_{susp} \quad (27)$$

for the downcomer:

$$\frac{F_{fr}}{A \cdot \gamma_L} = R_D = R_{fr} - R_{susp} \quad (28)$$

Addition of the two equations gives

$$2 \frac{F_{fr}}{A \cdot \gamma_L} = R_R + R_D = 2R_{fr} \quad (29)$$

The effect of the solid phase disappears if equation (27) and equation (28) are multiplied by $\frac{\gamma_L}{\gamma_m}$

$$2 \frac{F_{fr}}{A \cdot \gamma_m} = (R_R + R_D) \frac{\gamma_L}{\gamma_m} \quad (30)$$

where γ_m is the specific weight of the mixture and $R_R \frac{\gamma_L}{\gamma_m}$ and $R_D \frac{\gamma_L}{\gamma_m}$ the readings in head of mixture.

Subtraction of equation (27) and equation (28) gives

$$0 = R_R - R_D = 2R_{susp} \quad (31)$$

Substituting R_{susp} for $L \left(\frac{\gamma_s - \gamma_L}{\gamma_L} \right) c$ gives

$$R_R - R_D = 2 L \left(\frac{\gamma_s - \gamma_L}{\gamma_L} \right) c \quad (32)$$

With equation (30) we can express the flow rate and with equation (32)

we can express the concentration.

1.25 Summary. A mere addition of the manometer readings in head of mixture gives information on the friction loss across with vertical sections. The frictional loss in itself provides information on the flow rate of the mixture.

The subtraction of the readings of the manometers indicates a linear increase in concentration. Equation (32) states, that the manometric difference between two elevations is equal to the immersed weight of the material held in suspension between these two elevations. Equation (30) and Equation (32) are compared with experimental data in part 3 of this chapter.

2. Experimental Data

In Chapter III the experimental equipment and procedure was discussed. The sand used in the tests are described as follows:

2.1 Properties of the Solid Phase

2.11. Sand No. 2. In most experiments a Monterey sand Lapis Lustre No. 2 was used. For determining the specific weight, the formula $\gamma_s = W_s/V_s$ was used. For seven samples an overdry weight W_s was determined. The volume V_s was measured in a calibrated cylinder filled partially with water, by taking the displaced liquid as V_s . The ratio of W_s/V_s was found to be 2.607 kg/L. The ratio of wet weight to dry weight was found to be 1.15. A sieve analysis (Fig. IV-4) showed that d_{50} was 1.15 mm and that the sand was fairly uniform.

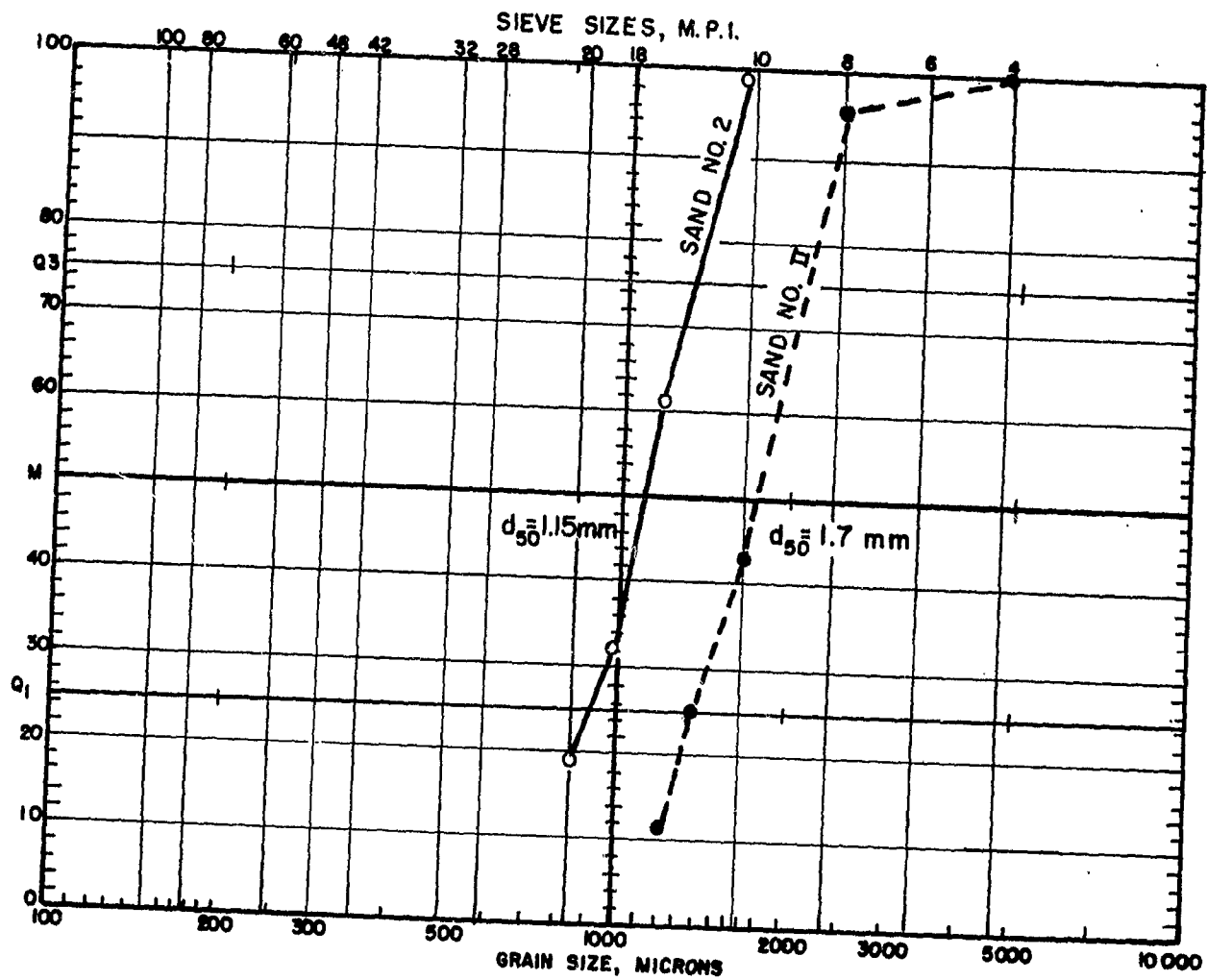


FIGURE N-4 - MECHANICAL ANALYSIS OF
SAND NO.2 & SAND NO. II

H9001A

2.12. Sand No. II. This sand was only used in a few experiments. The specific weight was determined by the previous procedure and was found to be 2.726 kg/L. The ratio of wet weight to dry weight was 1.04. The sieve analyses shown in Fig. IV-4 gave $d_{50} = 1.7$ mm.

2.13. Summary of Sand Characteristics. The characteristics of the sands used in the tests are summarized in the following Table IV-1.

| Sand | γ_s kg/L | d_{50} mm | $\frac{\text{wet weight}}{\text{dry weight}}$ | V_{Settl} m/s |
|--------|-----------------|-------------|---|------------------------|
| No. 2 | 2.607 | 1.15 | 1.15 | 0.11 |
| No. II | 2.726 | 1.70 | 1.04 | 0.16 |

Table IV-1

2.2 Experimental Procedure.

The experimental equipment was previously described in Chapter III. The discharge line was arranged in a Loop form. This means that after a 20 inch horizontal section there was an elbow and then a 90 inch vertical riser section. After another elbow, a short 52 inch horizontal section, and then it dropped again in a 90 inch vertical section to the original elevation. Figures III-1 and III-2 show views of the equipment.

The head difference across the vertical sections was desired. It was obtained in both cases over a section of 1.5 m. The pressure taps were here as high as possible in the riser to avoid elbow effects as much as possible. In the second vertical section the pressure taps were at an elevation as low as possible. The pressure measured at any lo-

cation was an average obtained from two opposite pressure taps.

2.21 Regulation of Flowrate. The discharge in the test section was regulated by a valve in the jet pump drive line. Thus, one could obtain various pressures in the jet chambers. This was the most effective device to change the flow rate in the experimental pipe without wear in the valve. As one might expect, also by increasing or decreasing the concentration the flowrate was slightly affected at a given setting of the valve.

2.22 Regulation of Concentration. The concentration in the experimental pipe was regulated by increasing or decreasing the total sediment content of the system.

2.23 Manometer Readings. The head across both vertical pipe sections was obtained by two 40 inch long air-water manometers. Every set of runs was started with clear water, i. e.: zero concentration. The reading on both manometers were the same, as expected. Then gradually the concentration was increased and it was noticed, that at the riser section the reading increased and at the downcomer section the reading decreased and in some instances gave negative values. This behavior is in accordance with the theoretical expectation as discussed in part 1 of this chapter.

The manometer scales were graduated in 1/100 of a foot, the 1/1000 ft was estimated. Minor fluctuations always existed. They were damped by friction in the saran tubing and by keeping the petcocks on the manometers only partially open. At some intermediate concen-

trations, and at certain flow rates the damping was not sufficient and an average had to be estimated. It is believed that this is a problem of instability when the solid phase probably moved in clouds.

The manometers were read before and after samples of the mixture were taken. The sampling procedure is explained in section 2.24. The difference in the manometer readings before and after sampling was small, since the sampling time was short. The averages of the readings were then determined for each vertical section.

The readings for the riser and downcomer section are tabulated in column 4 and 5 of Appendix I.

2.24 Sampling Procedure. The sampling of sediment was accomplished after equilibrium was reached, i.e., when the concentration remained constant. This could be checked on the manometer readings. The sample was taken from the flow by means of a three-way valve, which diverted the flow for a desired time into a weighing tank. The weighing was done as described in Chapter III. The sampling time used in the experiment ranged from 0.8 seconds to 2.2 seconds. The reason for the short sampling time, was to prevent an excessive decrease of concentration in the system. The weight in kg of mixture, of sand and of water then was recorded. The weight in kg of mixture ranged from 10 kg to 17 kg and the weight in kg of sand from 0 kg to 6.5 kg.

2.3 Determination of Flow Rate and Concentration

2.31 Determination of Flow Rate: The flow rates were determined from the sampling weights and times. Since the weight of sand

was obtained as a wet weight, the values had to be corrected to dry weight. The correction factor is given in Table IV.1. In the same table γ_m is given for both sands. Dividing the dry weight by γ results in the volume. The flowrate was obtained by dividing the volume by the time, and then presented in liter/sec. The flow rates are given in column 1 of Appendix 1.

2.32 Determination of Concentration: We want to have the concentration in volume percentage. This was obtained as the ratio between sediment flow rate and total mixture flow rate. This was done for each run and is tabulated in column 7 of Appendix 1.

2.4 Summary of Experiment

From our experiment we obtained the readings at an air-water manometer in head of water for the riser and the downcomer section. Furthermore, the flowrate of the mixture was obtained in liters per seconds and the concentration in volume percent. These four values are tabulated for each run in Appendix 1.

3. Comparison of Experiment and Theory

3.1 The Concentration

We shall now compare the experimental results with equation (32). Rewriting this equation gives

$$R_R - R_D = 2 \cdot L \cdot \left(\frac{\gamma_S - \gamma_L}{\gamma_L} \right) \cdot c \quad (32)$$

The value (2L) is 3 meters. R_R and R_D are obtained as manometer readings in head of liquid.

For the two different sands $\left(\frac{\gamma_S - \gamma_L}{\gamma_L} \right)$ was 1.607 for sand No. 2

and 1.726 for sand No. II. Using these experimental values we obtain

for sand No. 2

$$R_R - R_D = 4.821 c \quad (33)$$

for sand No. II

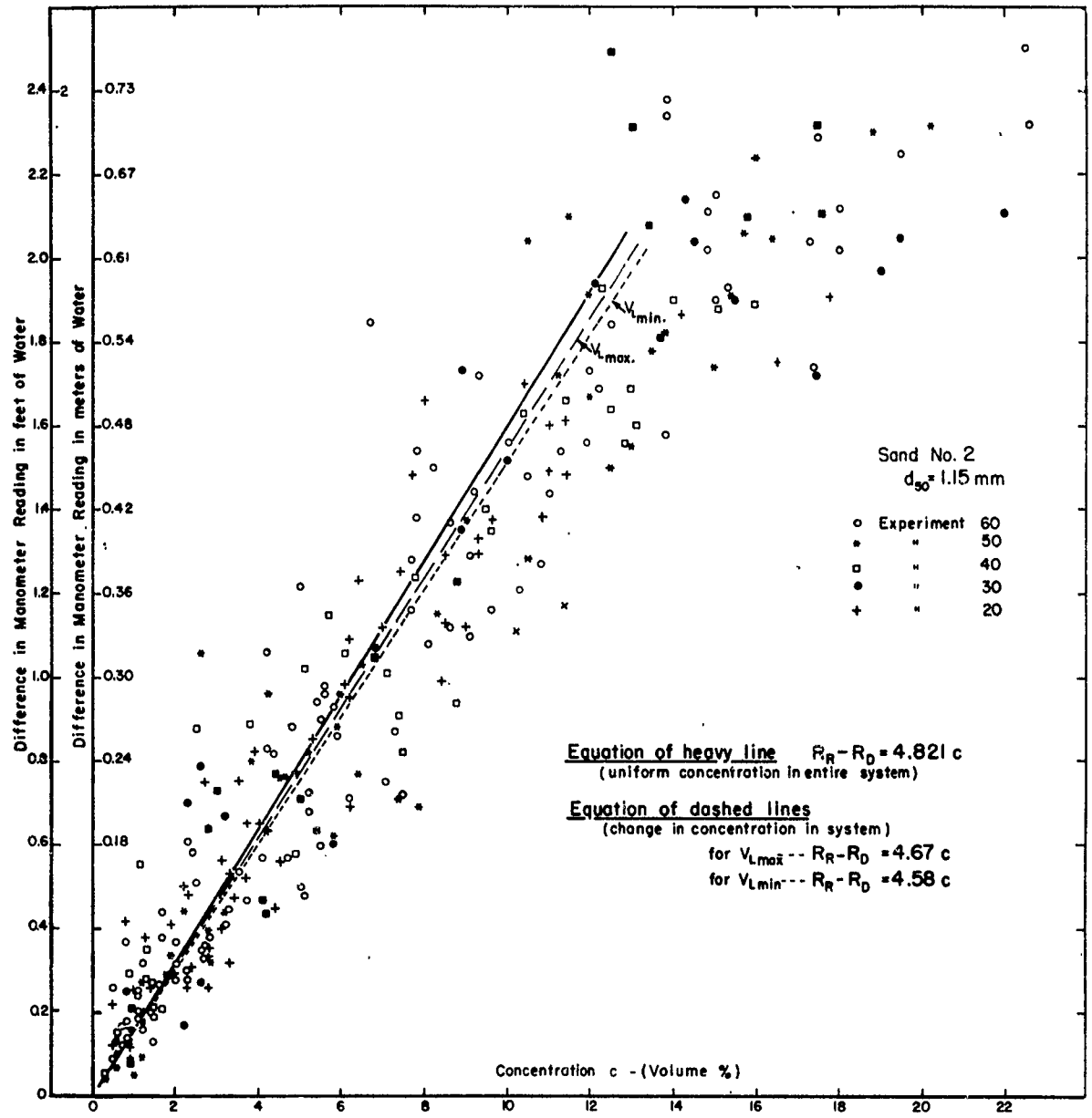
$$R_R - R_D = 5.178 c \quad (34)$$

Both equations plot as straight lines for $R_R - R_D$ versus concentration. Equation (26) is plotted in Fig. IV-5. Also in this figure are plotted about 350 experimental values for sand No. 2. It is apparent that the experimental data fit the theoretically line quite well despite of the rather large scatter. This is especially true at the lower and intermediate concentrations, but at higher concentrations (> 12%) the experimental data may deviate systematically somewhat from the predicted line. No explanation is given for this. In Fig. IV-6, the experimental runs with sand No. II are compared with equation (34). Also here it is noticed, that the data are in good agreement with the theoretically predicted line. The experimental data used in Fig. IV-5 and Fig. IV-6 are tabulated in Appendix 1. For these two figures it was necessary to calculate the differences of the two manometer readings at the riser and at the down-comer section, as tabulated in column 6 of the Appendix 1, starting with zero at zero concentration and increasing with concentration.

3.2 The Flow Rate . The theoretical equation derived in part 1 of this chapter is:

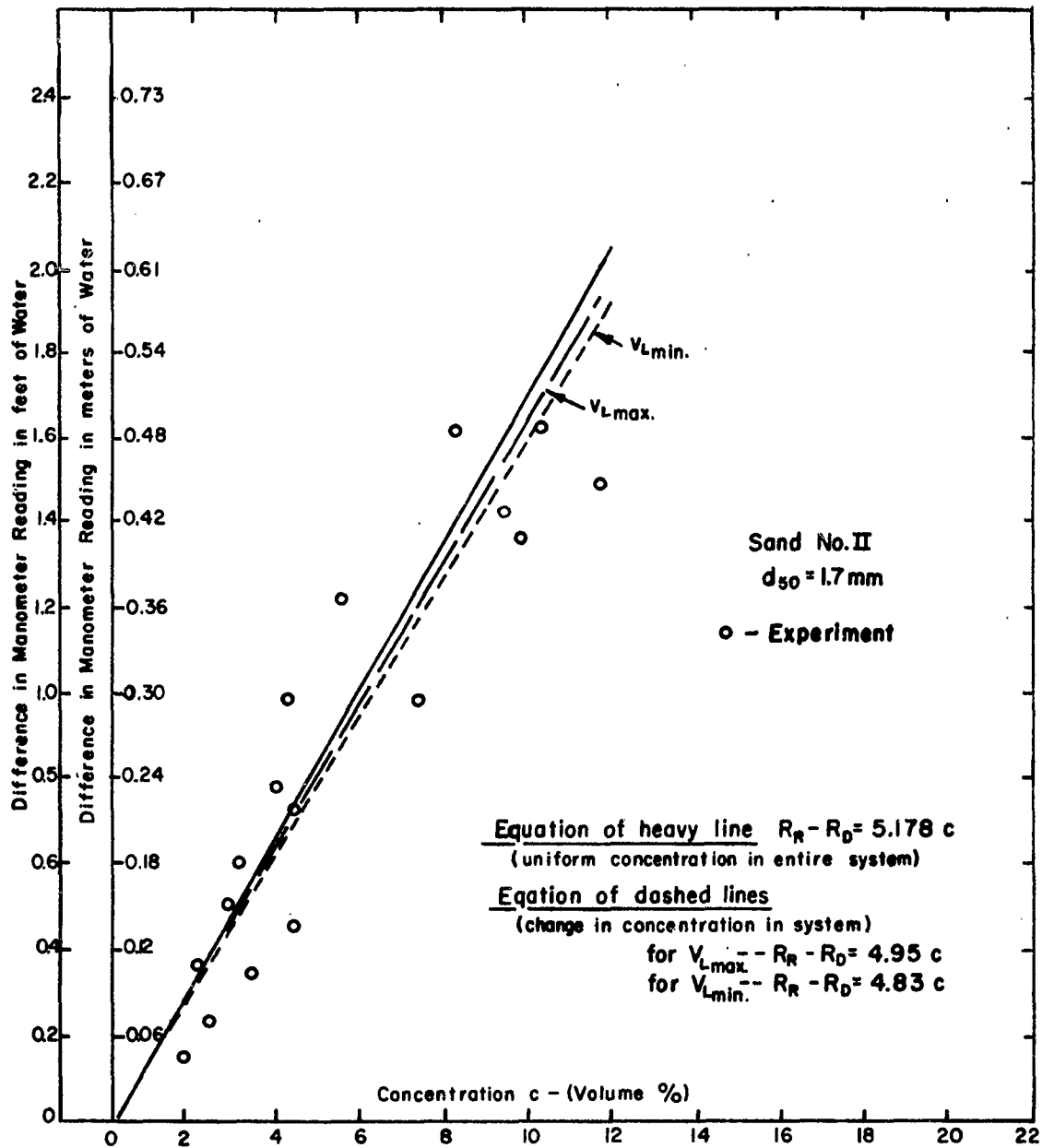
$$2 \cdot \frac{F_{fr}}{A \gamma_m} = (R_R + R_D) \frac{\gamma}{\gamma_m} \quad (30)$$

The right side of this equation is the manometer reading in head of mix-



H9003C

FIGURE IV - 5 - CONCENTRATION vs MANOMETER READING DIFFERENCE
 LOOP SYSTEM [Volume %] vs [Meters or Feet of Water]



H9003C-a

FIGURE IV-5a- CONCENTRATION vs MANOMETER READING
 DIFFERENCE (Volume %) vs (Meters or Feet of Water)
 LOOP SYSTEM

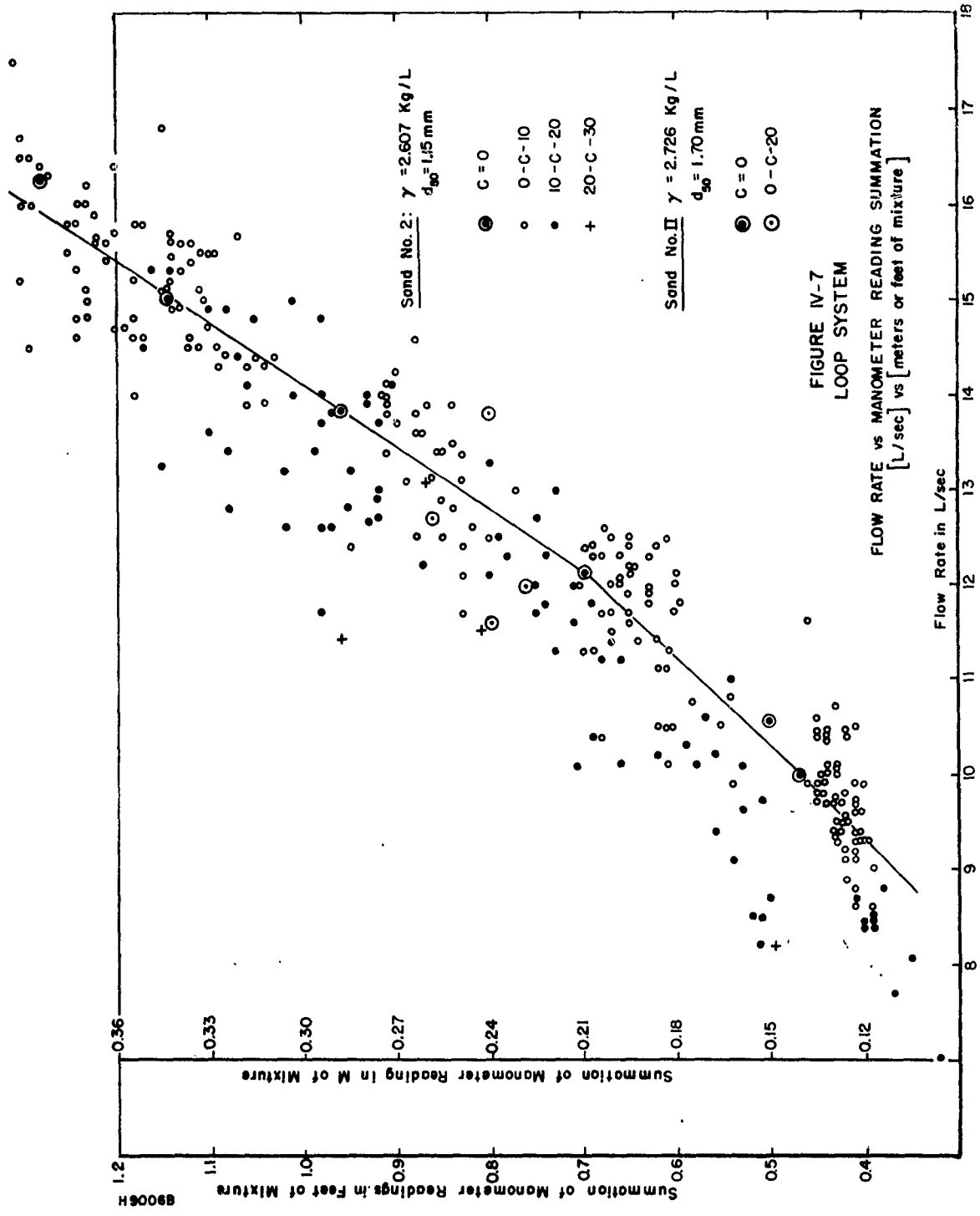
ture. This value of $(R_R + R_D)$ was determined for each run and is shown in column 3 of Appendix 1 in head of water. The values of this term were multiplied by γ/γ_m and tabulated in column 2, Appendix 1. The specific weight of the mixture was obtained as follows:

$$\gamma_m = \gamma_L + (\gamma_S - \gamma_L) c \quad (31)$$

The left side of equation (30) is the friction loss over both the riser and the downcomer sections. The frictional loss is generally speaking proportional to the square of the velocity and flow rate. Therefore, the right side of equation (30) was plotted versus the flow rate. The circled points shown in Fig. IV-7 were obtained for clear water. All other points represent various concentrations. They show some scatter around the line for clear water. On Fig. IV-7 experimental values of both sands are plotted. It is expected that the points follow on a log-log paper a line with an approximate slope of 2. This is shown on Fig. IV-8, where the slope of the best fitting straight line of Fig. IV-7 was 2.17.

3.3 Confirmation of the Assumption of Constant Concentration in Entire Loop System:

That the concentration in the riser and in the downcomer section are equal was assumed in part 1.23 of this chapter and is proved as follows; by applying the continuity equation for the solid phase in the riser and the downcomer section. Therefore, the same amount of discharge which first goes up in the riser section must then come down the downcomer section. We write therefore,



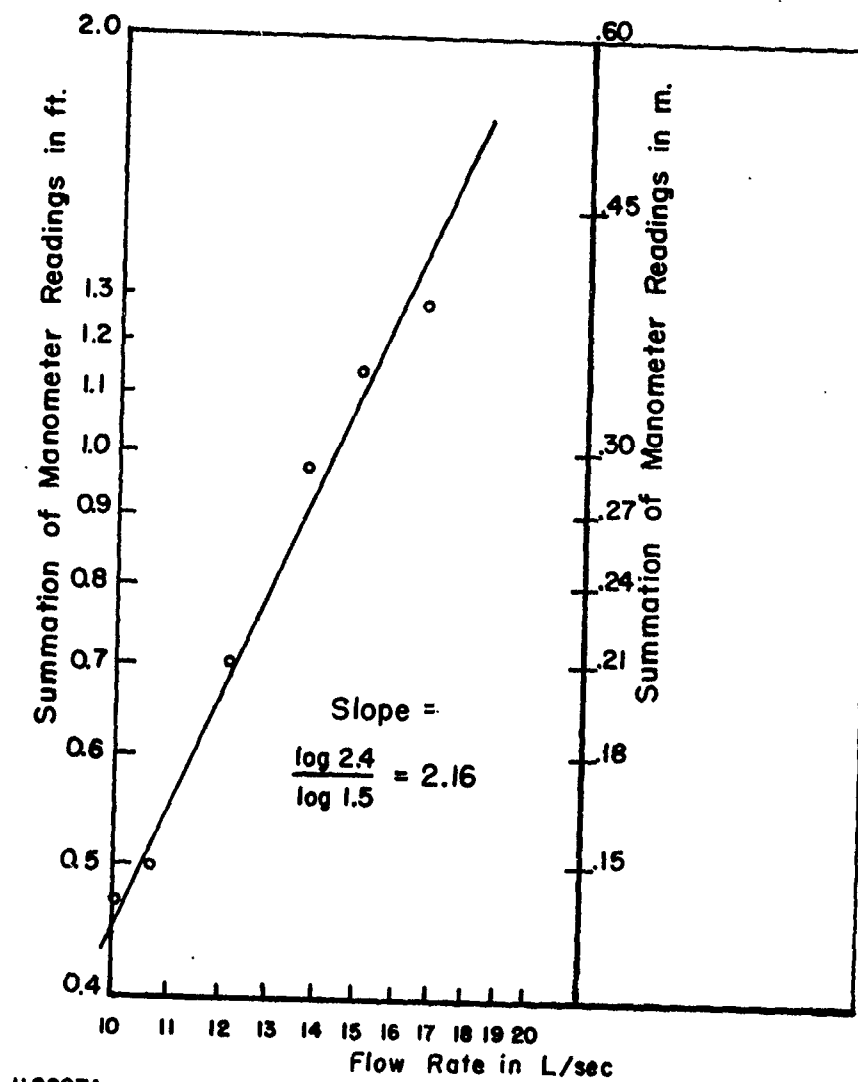


FIGURE IV-8 - LOOP SYSTEM
 SUMMATION OF MANOMETER READINGS (meters)
 vs FLOWRATE (L/sec)
 for clear water

$$Q_s, \text{ in riser} = Q_s, \text{ in downcomer} \quad (35)$$

For Q_s we use equation (1) which combined with equation (35) gives

$$(A \cdot c \cdot v_s)_{\text{in riser}} = (A \cdot c \cdot v_s)_{\text{in downcomer}} \quad (36)$$

The area A appears on both sides therefore equation (36) reduces to

$$(c \cdot v_s)_{\text{in riser}} = (c \cdot v_s)_{\text{in downcomer}} \quad (37)$$

The solid phase velocity in the riser section can be expressed according to Fig. IV-2 as being

$$v_s \text{ in riser} = v_L - v_{\text{settl}}$$

This means that the solid phase will move slower than the liquid phase by an amount of its settling-velocity. From Fig. IV-3 we may obtain that in the fall section the sand velocity will be larger by the amount of the settling velocity. Then we write:

$$v_s \text{ in downcomer} = v_L + v_{\text{settl}}$$

Combining equation (38) and equation (39) with equation (37) we obtain

$$\frac{v_L - v_{\text{settl}}}{v_L + v_{\text{settl}}} = \frac{c_D}{c_R} \quad (40)$$

Where c_D is the concentration in the downcomer section and the concentration in the riser section is c_R . The influence of the settling velocity will cause the deviation of c_R from c_D . By means of numerical values, taken from the experiments, it is shown, that the concentration does not change significantly in the entire Loop system. The following table (Tab. IV-2) illustrates this fact for the two sands used in the tests.

Table IV-2

| | | | |
|----------------|---------------------------------------|---------------------------------------|-------------------|
| Sand No. 2 | $v_{\text{settl}} = 0.11 \text{ m/s}$ | $v_{L \text{ max}} = 3.7 \text{ m/s}$ | $c_D/c_R = 0.945$ |
| | | $v_{L \text{ min}} = 2.2 \text{ m/s}$ | $c_D/c_R = 0.905$ |
| Sand No. II | $v_{\text{settl}} = 0.16 \text{ m/s}$ | $v_{L \text{ max}} = 3.7 \text{ m/s}$ | $c_D/c_R = 0.920$ |
| | | $v_{L \text{ min}} = 2.2 \text{ m/s}$ | $c_D/c_R = 0.866$ |

The maximum and minimum test velocities were selected. All other values will be found between this two extreme velocity values. We now replace c in equation (32) by $(c_R + c_D) \cdot 1/2$ and will investigate how far this affects equations (26) and (27). Also this is summarized in Table IV-3.

Table IV-3

| Sand | Velocity | If $c_D = c_R$ | If Assumed no Change in Concentration in the Whole Loop, i.e. $c_D = c_R$ |
|--------|------------------|----------------|---|
| No. 2 | V_{max} | $4.67 c$ | $4.821 c$ |
| | V_{min} | $4.58 c$ | (Eq. 33) |
| No. II | V_{max} | $4.95 c$ | $5.178 c$ |
| | V_{min} | $4.83 c$ | (Eq. 34) |

From Table IV-3 we conclude, that at the small liquid velocities, the deviation from the equation (33) or equation (34) are the largest, yet this deviation is quite small. It can be observed by examination of Fig. IV-4 and Fig. IV-5, that our assumption of a uniform concentration all through the Loop system was justified, and the effect of the settling velocity is

of insignificant influence in this investigation.

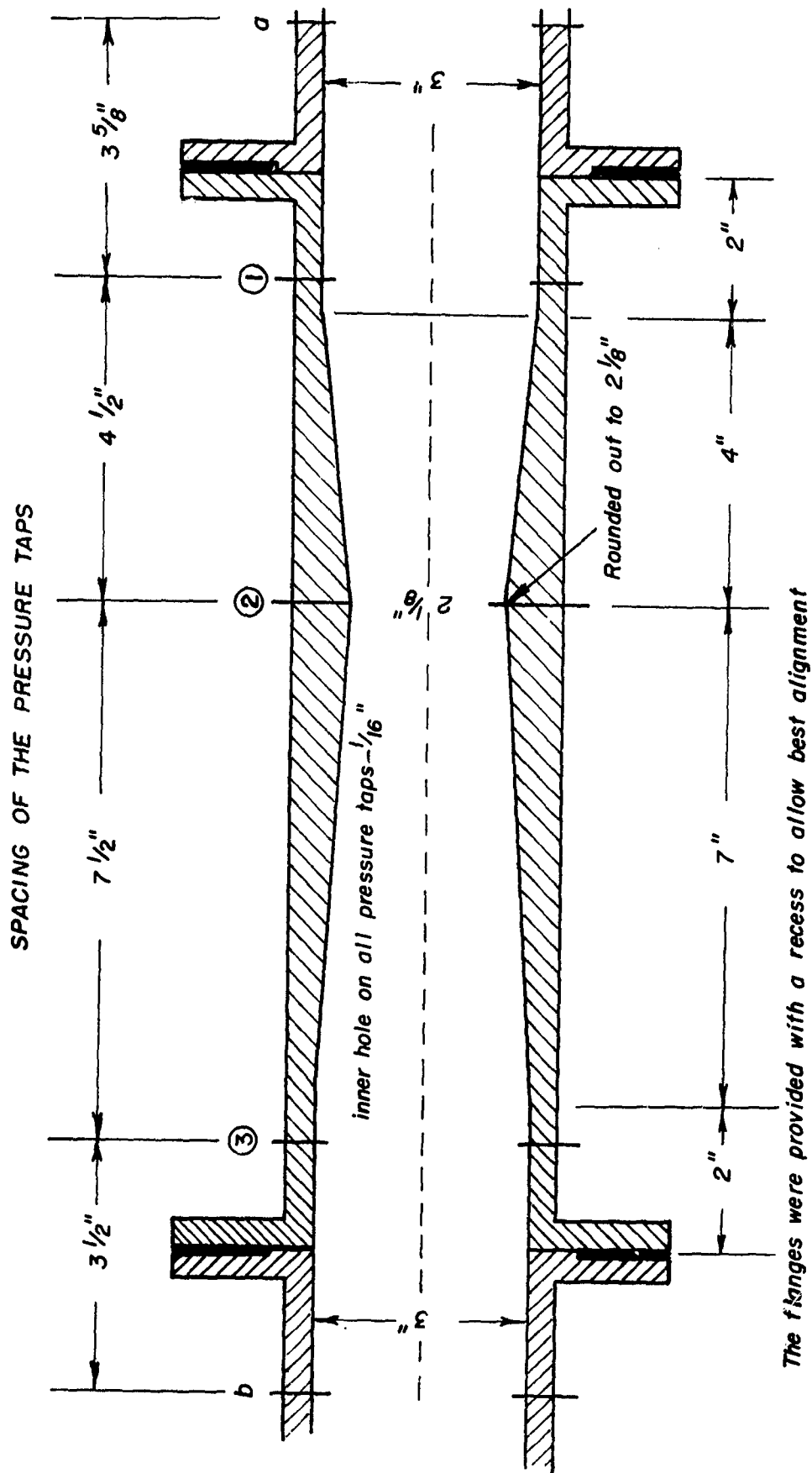
V. VENTURI METER

In chapter IV the Loop system was considered. A successful result was expected and the expectation was satisfied since it permitted the determination of the flowrate and the concentration by manometer readings only. But the Loop system, due to its rather awkward shape, might not be the best for practical purposes. For this reason another design was investigated. It was a modified Venturi meter.

1. Experimental Results

The applicability of a Venturi meter in a two-phase flow problem is considered. We know that in a single-phase flow the pressure drop in the contracted section can be correlated with the flow rate. In order to obtain some additional information on the concentration additional measurements were needed. As such it was decided to obtain in the two-phase flow problem the head-loss across the Venturi meter; however, it is necessary to explain the experiment in order to establish a theory.

The Venturi meter as used (see Fig. III-1) was placed in a horizontal section of the 3 inch pipe line system. The throat diameter of the Venturi was 2-1/8 inches. A longitudinal section through the Venturi is shown in Fig. V-1. The Venturi meter was especially machined for this purpose and special care was taken to obtain a smooth transition from the pipe to the Venturi. The pressure drop was recorded between tap locations (1) and (2) by means of an air-water manometer. The head difference, converted into head of mixture, was then plotted in

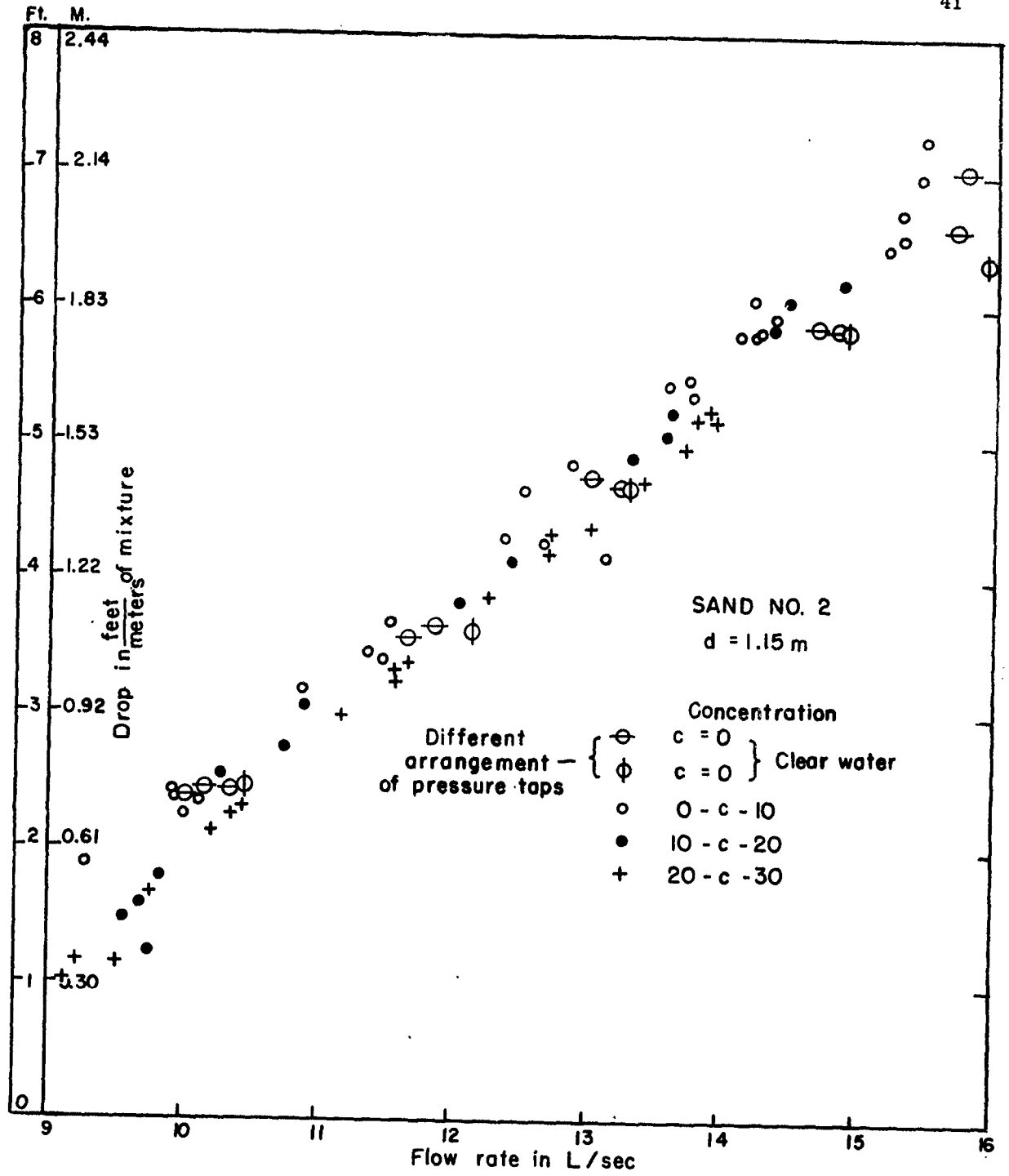


H 8995A

FIGURE V-1 - CROSS SECTION THROUGH VENTURI METER

graph Fig. V-2 and 2A versus the flow rate and is also tabulated in Appendix 2. The points for the various concentrations fell on the clear waterline for sand No. 2, as may be seen. For Sand No. II they do not seem to correlate quite as well with the clear water line, especially for the high concentrations. In Fig. V-3 the clear water line is replotted on log-log paper and seems to follow quite well a straight line with the slope 2.26. This is in accordance with the theory, that for turbulent flow any head difference is proportional to the square of the velocity, as long as the sediment motion deviates only insignificantly from that of the water.

Another reading was obtained, which indicated the energy-loss across the Venturi meter. The pressure-taps (a) and (b) (see Fig. V-1) were used for this purpose. To avoid any local effect of the Venturi meter the pressure taps were located about 4" away from the beginning and the end of the taper. This seems to be quite important in the downstream section, where we must take the possibility in account that some separation could occur. This was checked, by having a series of pressure taps along the exit of the Venturi meter. After study of the results, obtained with different concentrations, it was decided to use tap (b). The head-loss across the meter between (a) and (b) was measured by another air-water manometer. The reading may be called "b". It was observed that "b" increased with concentration. For this reason "b" was plotted against concentration and the flow rates noted at all points (Fig. V-4 and 4A). The values of "b" and concentration c are tabulated in Appendix 2. One is able to draw through the different experimental



H8996A

FIGURE V-2 - VENTURI METER
Drop vs. Flow Rate

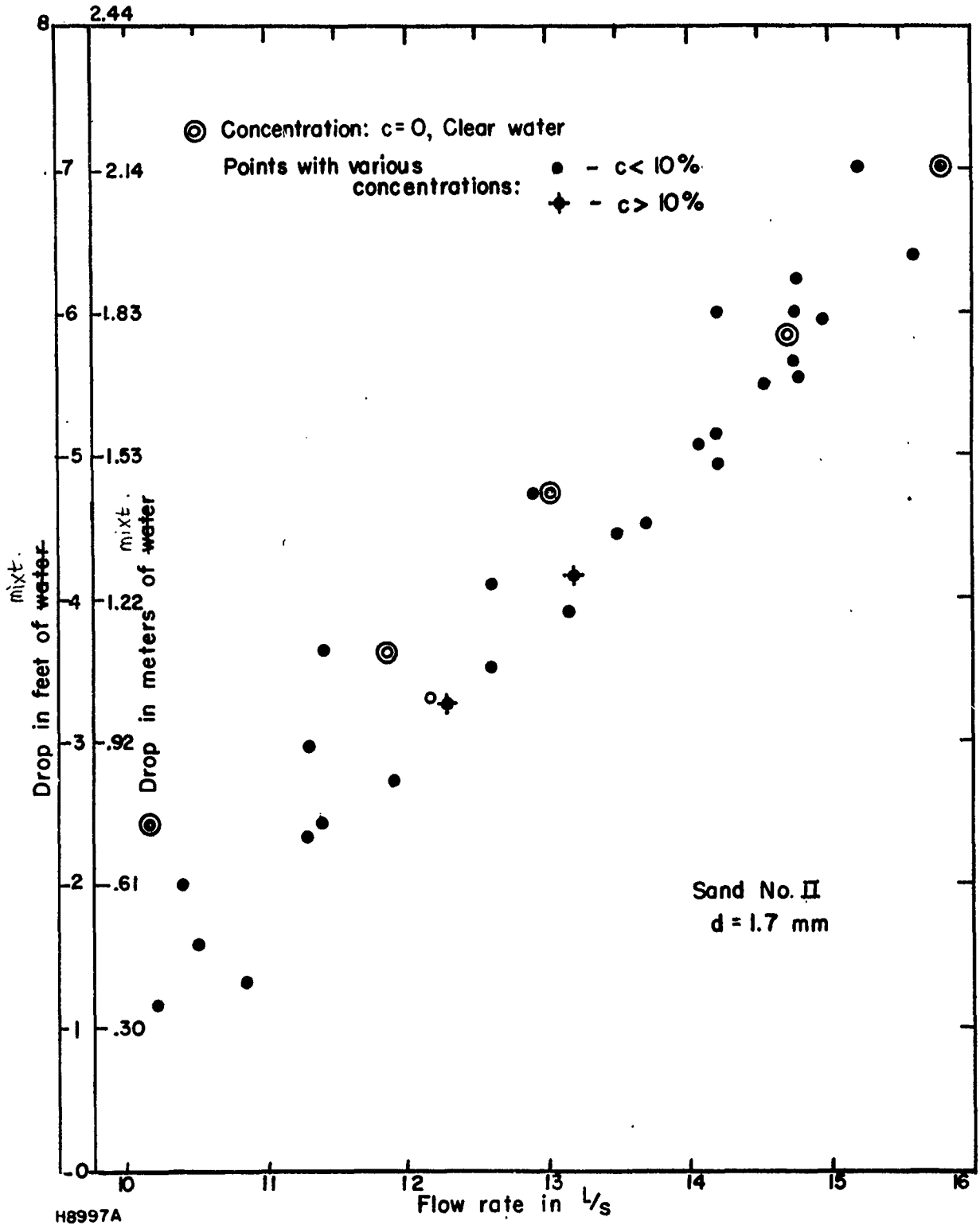
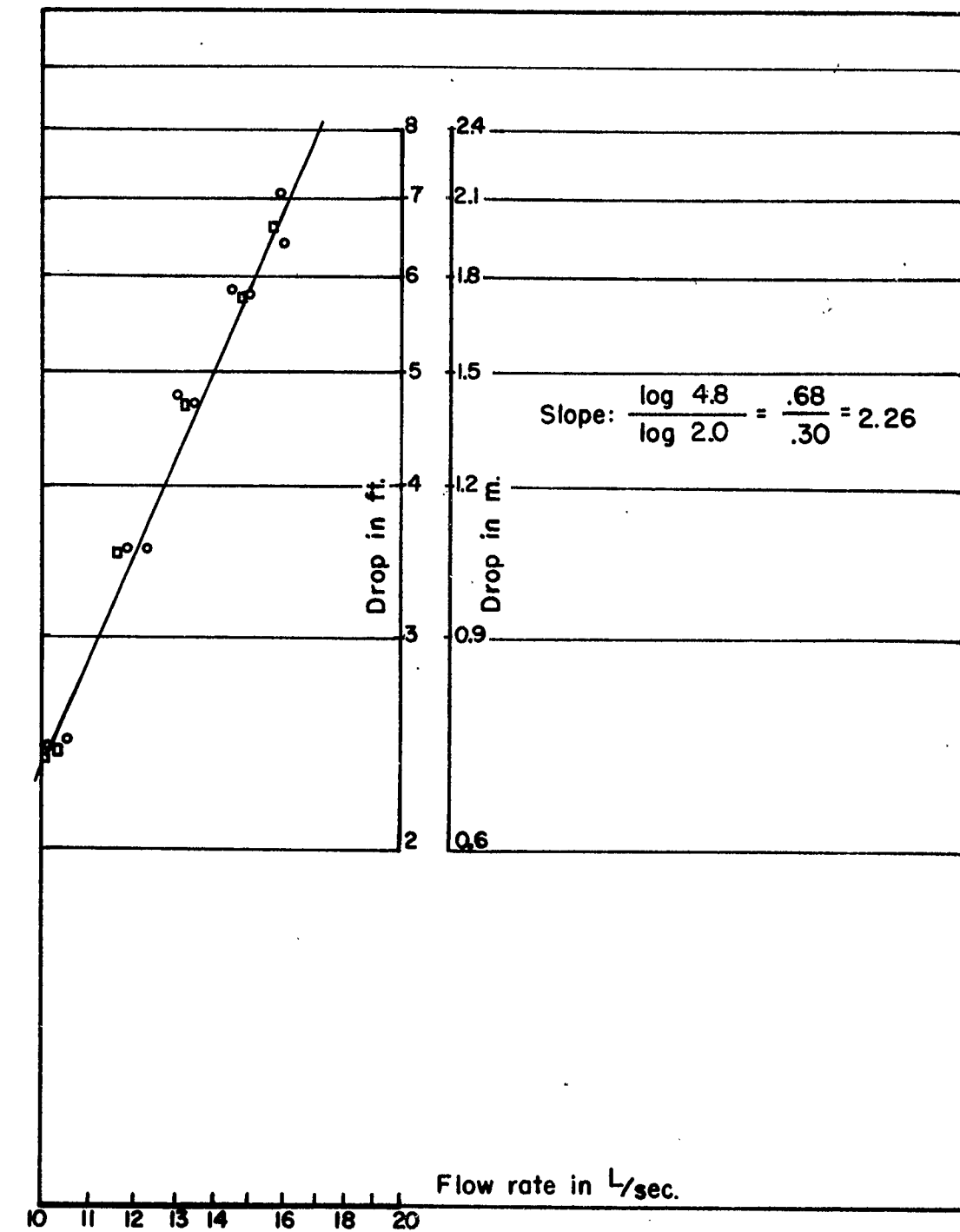


FIGURE V-2A - VENTURI METER
 Drop vs Flow Rate

H8997A



H8998A

FIGURE V-3 - VENTURI METER
Drop (m. or ft.) vs Flow Rate (L/sec.)

points lines of equal flow rate or equal velocity. All of these equal-flowlines, ranging from $9\frac{1}{2}$ l/sec to 15 l/sec, have the same slope. We now assume that the losses through a venturi due to contraction, expansion and wall friction are just a function of the velocity. This part of the loss shall be called " b_0 ". " b_0 " may thus be determined as the energy loss at zero concentration and shall be subtracted from the total loss " b ". The remainder " $b-b_0$ ", tabulated in Appendix 2, was plotted in Fig. V-5 against concentration. This graph shows that regardless of the flow rate the value " $b-b_0$ " is uniquely related to the concentration.

We shall go back to Fig. V-4 and 4A and reason, why some of the points do not follow the equal flow rate lines. It was observed at pressure readings just upstream of Venturi meter that the velocities increased by adding more solid material. This means, that at a low velocity the water is unable to carry all of the solid phase. Part of it settles and causes a decrease in cross section, which may be recorded on a manometer as an increase in velocity. On the other hand the material which accumulates on the bottom of the pipe will not pass through the Venturi meter and therefore the head " $b-b_0$ " is expected to decrease, and also the concentration should decrease. The first effect, a decrease in " $b-b_0$ " can be seen clearly in Fig. V-4 and 4A. The second effect a decrease in the concentration moved through, does not show in the graph of Fig. V-4 and 4A. This is due to the fact, that the concentration plotted is the fraction of solid phase involved in the investigation. By comparing Fig. V-4 and Fig. 4A we notice, that in Fig. V-4A accu-

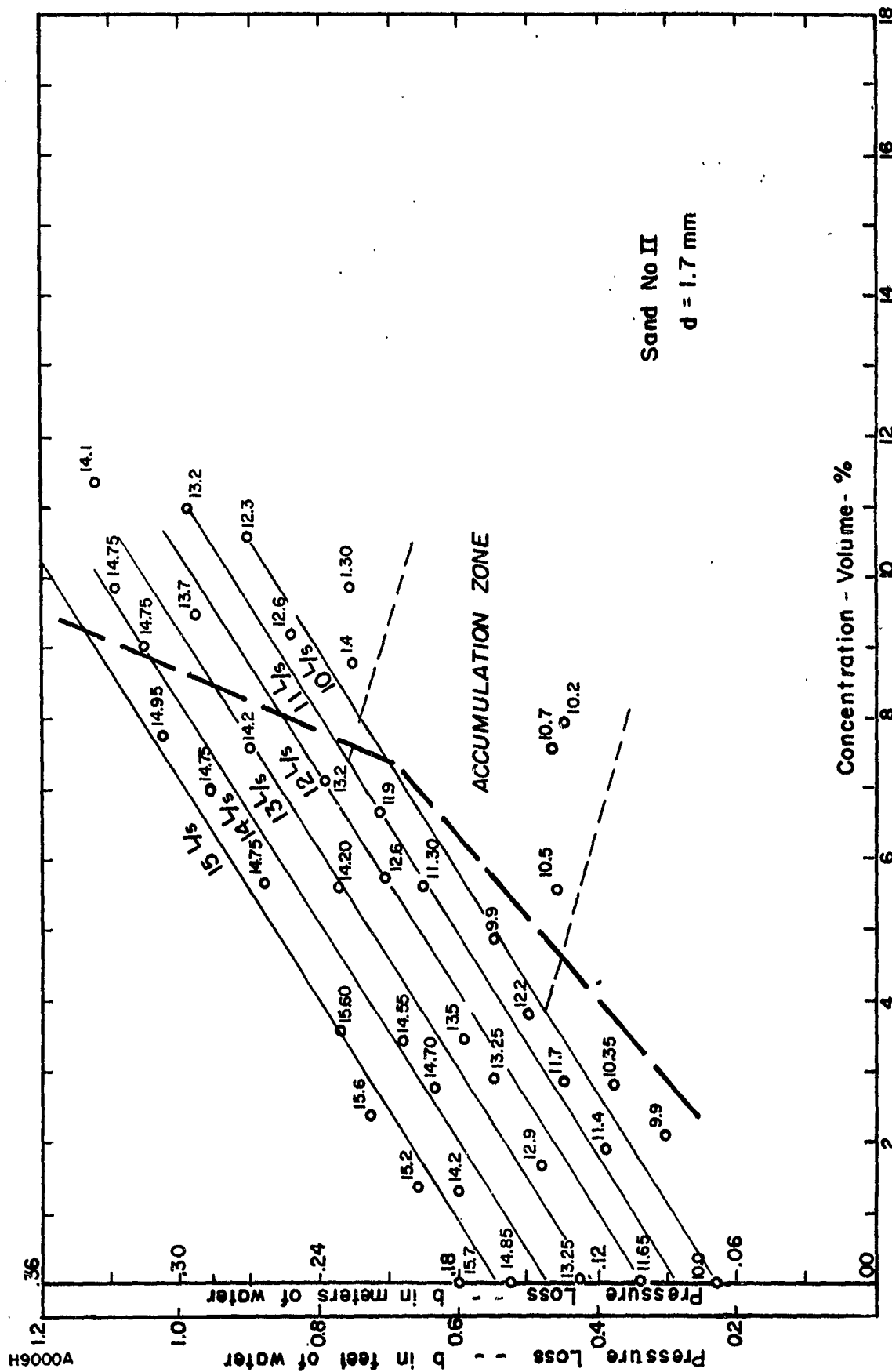


FIGURE V-4A - VENTURI METER
Pressure Loss vs Concentration

mulation occurs at lower flow rates. The reason of this probably is due to the larger grain size.

From Fig. V-5 we can obtain the relationship between "b-b₀" and the concentration. This is

$$(b-b_0) = 1.95 \cdot l_v \cdot c \quad (41)$$

Here l_v is the length over which "b-b₀" is recorded and is a geometric constant of the particular instrument.

c is the concentration and 1.95 is a dimensionless parameter. This parameter may be expected to change with the type of sediment, but the experimental results indicated the same parameter for both kinds of sand, with a slight variation in diameter ($d_{50} = 1.15$ mm and 1.7 mm) and in density ($\gamma = 2.60$ kg/L and 2.72 kg/L), it is believed that this parameter is a function of grain geometry as well as of the density. Further research must develop this relationship. In addition to the fact that the parameter could change with the characteristics of the material, it will also change with geometry of the Venturi meter, i. e., with the ratio A_1/A_2 and l_v .

The experiment described above was done with water as the liquid phase and sand No. 2 and No. II as the solid phase. As stated in Chapter IV, the sand No. 2 had a mean diameter of 1.15 mm, the other one had a mean diameter of 1.7 mm. It should also be mentioned, that the flow rate and the concentration were obtained by the calibrated Loop system, which was arranged in series with the Venturi. This arrangement accelerated the process of obtaining the experimental data.

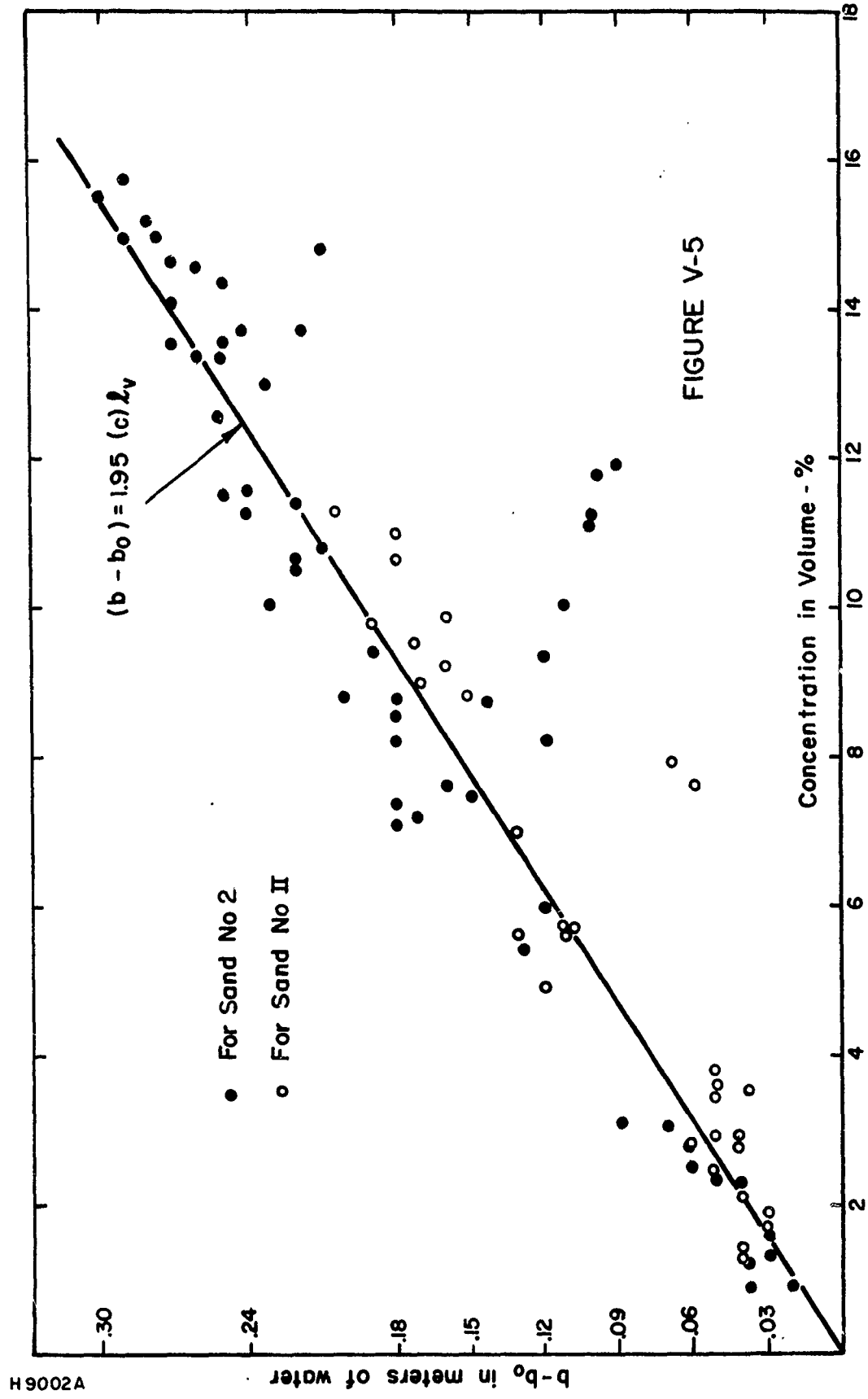


FIGURE V-5 - VENTURI METER
 b - b₀ (meters) vs Concentration-(Vol.%)

2. Theory

2.1 The Pressure Drop

We shall try to develop a theoretical explanation, why the pressure drop reading caused by the flow of a mixture in a Venturi permits determination of the flow rate. For this purpose let us consider Fig. V-6α. We will assume that the Venturi has a horizontal axis and that the

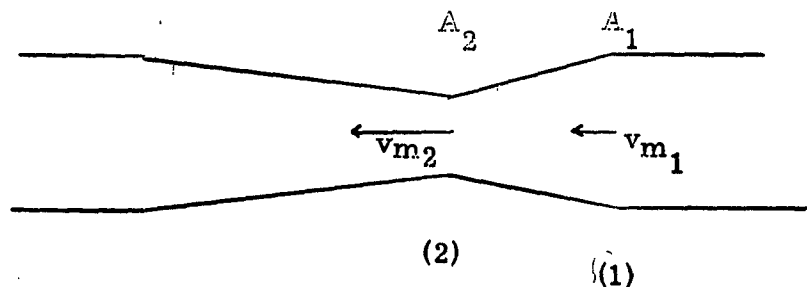


Fig. V-6α

mixture is incompressible. Furthermore, we shall assume that the concentration will not vary from cross section A_1 to cross section A_2 . We shall neglect frictional effects and assume a uniform velocity distribution at the inlet and at the throat. In such a case the energy equation for steady flow gives the relation:

$$\frac{p_1}{\gamma_m} + \frac{v_{m1}^2}{2g} = \frac{p_2}{\gamma_m} + \frac{v_{m2}^2}{2g} \quad (42)$$

where p_1 and p_2 are the heads in points (1) and (2), γ_m is the specific weight of the mixture and v_m is taken to be the velocity of the mixture.

In addition to the energy-equation we can use the continuity equation, which reads:

$$Q_m = v_{m1} A_1 = v_{m2} A_2 \quad (43)$$

here Q_m is the total flow rate.

Combining equation (42) and (43) we obtain

$$Q_m = C_v \frac{A_2}{\sqrt{1-(A_1/A_2)^2}} \cdot \sqrt{\frac{2g(p_2 - p_1)}{\gamma_m}} \quad (44)$$

Since the derivation has been done for an ideal fluid, the factor C_v stands for additional real fluid effects and approaches 0.98 at high Reynolds numbers. Equation (4) could be rearranged so that it reads:

$$Q_m = \left[C_v \frac{A_2}{\sqrt{1-(A_1/A_2)^2}} \cdot \sqrt{2g} \right] \cdot \sqrt{\frac{p_2 - p_1}{\gamma_m}} \quad (45)$$

The bracket term on the right side of this equation is a constant for our experiment, and the term $\frac{p_2 - p_1}{\gamma_m}$ is equal to the head of mixture.

This is good for the turbulent flow and we see immediately from equation (45) that $Q_m^2 \sim a_m$, where a_m is the pressure drop in meters of mixture.

As a summary we can say that the laws which explain the Venturi effect in a liquid, also explain the flow of a mixture through a Venturi meter, if certain assumptions are made. The pressure-drop reading has to be taken in terms of the mixture.

The experimental results, tabulated in Appendix 2 and plotted in Fig. V-2 and 2A seem to prove this. The slight systematic deviations in Fig. V-2A indicate, however, that the concentration as well as the solid particle size has to be studied more extensively.

2.2 Energy Loss

2.2.1 The Drag Equation . An attempt shall be made to explain the energy loss across the Venturi meter . In Fig. V-4 and 4A the total energy loss is plotted against concentration . This total energy loss may be called "b" . It includes the frictional loss , the losses due to contraction and expansion and a certain loss due to the solids . Furthermore, it was shown in part 1 of this chapter , that under the assumption that the friction-expansion- and contraction losses are linearly superimposed on the concentration effect, these two effects can be separated . In Fig. V-5 this was done and it is seen, that the effect due to the concentration is in this investigation independent of velocity or flow rate with the velocities ranging from a maximum of 4 m/sec to a minimum of 2 m/sec . The relationship between the head and the concentration c was established in equation (41);

$$(b-b_0) = 1.95 \cdot \ell_V \cdot c \quad (41)$$

The solid particles had been assumed to move with the same velocity as the liquid phase in the case of steady flow . This is to say, that there exists no relative motion between the two phases . In the Venturi meter we have significant accelerations with the corresponding pressure gradients . Since the mass of a solid particle is bigger, than that of the displaced fluid, its acceleration in a pressure gradient will be smaller than that of the liquid . This will cause a relative motion between the solid and liquid phase . This relative motion will be different in each cross section of the Venturi meter . A certain amount of energy is necessary to main-

tain this relative motion. And this seems to be the additional energy-loss due to the presence of the solid phase. We shall express the resistance of the sand in water with a drag equation. Then we get:

$$(b-b_0) = \frac{\text{Drag}}{\gamma \cdot A} \quad (46)$$

A detailed examination of this drag equation shows that the relative motion changes throughout the Venturi or in other words the solid particle is accelerated with respect to the liquid. Obviously the steady-state drag equation is insufficient for this type of problem. The concept of virtual mass was established in the 18th Century. Later Bessel (Ref. 11) defined the virtual mass as being the mass of fluid displaced by a body multiplied by a factor k , the virtual mass coefficient. In Ref. 10 Prandtl and Tietjens explain this phenomenon as follows:

"For an accelerated motion, it was seen that potential flow does lead to a resistance. In order to accelerate a sphere in an ideal fluid it is not only necessary to exert a force equal to the product of the mass of the sphere and its acceleration, but an additional force is required to accelerate the mass of the fluid particles set in motion by it. From the above equation for the resistance, it is seen that this additional force is equal to the product of the acceleration of the sphere and the mass of an amount of fluid of half its volume. The apparent increase in mass of various bodies depends on the shape and on the direction of motion. For instance, for the two-dimensional flow around a circular cylinder, the apparent increase in mass is equal to the full mass of the cylinder in

liquid." For a number of other bodies the added mass coefficient is summarized in the paper by Iversen & Balent (Ref. 2). These added mass coefficients are of limited importance since the real fluid behaves differently than the ideal fluid. In 1924 Lunnon (Ref. 3 and Ref. 4) reported from his own experiment that this coefficient varied. His investigation with spheres showed a variation from $k = 0.5$ to $k = 2.0$, where the one obtained with potential flow was reported to be $k = 0.5$. Iversen & Balent (Ref. 2) reported in their paper, that their research on a disk resulted in an added mass coefficient of $k = 0.637$ to $k = 5.0$, where the lower value is the one obtained with potential theory. The same authors were able to obtain by dimensional analyses an "acceleration parameter" $\frac{A \cdot D}{V^2}$ and established fairly successfully a relationship between the added mass coefficient and this acceleration parameter. This result is shown in Fig. V-9. Also shown in the same graph are Bugliarello's (Ref. 5) research with spheres. The variation of the added mass coefficient was from $k = 0.4$ to $k = 100$. He failed to find any relationship between his k values and the acceleration parameter. With the few results available one may see the complexity of a problem dealing with non-steady flow.

We shall try to set up an equation for total drag. The steady state drag equation can be written as:

$$\text{DRAG}_1 = K_1 U_p^2 \quad (47)$$

Additional to this drag, we will have to introduce the acceleration drag.

This can be done in two ways.

The first way might be as follows: To the steady state drag, the acceleration drag has to be added and we get:

$$\text{Drag}_2 = K_1 U_p^2 + k(V_S \rho_L) \dot{U}_p \quad (48)$$

For a given body geometry, K_1 , in equation (47) and equation (48) is a function of Reynolds number and k shall be a function of the acceleration parameter. V_S is the displaced volume of liquid.

The second way to take in account the acceleration forces is to modify the steady state drag equation. In this case equation (47) is:

$$\text{Drag}_3 = K_3 U_p^2 \quad (49)$$

Here K_3 is not only a function of Reynolds number, but also of the acceleration parameter.

It seems reasonable to use equation (49) where the acceleration effect is of minor importance.

2.2.2 Equation of Motion. It was seen at the beginning of part 2.2.1 of this chapter, that there will be a relative motion between the solid and liquid phase throughout the Venturi meter. This relative velocity is responsible for the existing drag, or in other words it is responsible for the additional energy loss, which is termed "b-b₀". This relative velocity, averaged over the length of the Venturi meter where the loss obtained is to be determined. For this reason the differential equation is established for a solid particle being moved by the pressure gradients of the liquid and exerting a certain drag. The differential equation of motion is in such a case

$$\rho_S \cdot V_S \cdot \dot{v}_S = \rho_L \cdot V_S \cdot \dot{v}_L - \text{Drag} \quad (50)$$

For the drag equation (49) is introduced and \dot{v} is replaced by $v \frac{dv}{ds}$, since $\frac{\partial v}{\partial t}$ is zero. We obtain:

$$\rho_s \cdot V_s \cdot v_s \frac{dv_s}{ds} = \rho_L \cdot V_s \cdot v_L \frac{dv_L}{ds} - K_3 U_p^2 \quad (51)$$

U_p is the relative velocity and is replaced by $(v_s - v_L)$. Furthermore, the expression $\frac{1}{2} \cdot C_R \cdot A \cdot c \cdot \rho_L$ is substituted for K_3 , where C_R is a resistance coefficient and is a function of the Reynolds number, of the particle with respect to the surrounding fluid and of the acceleration parameter. Since the particles are always submerged, the Froude number does not influence the resistance coefficient. Introducing these substitutions and writing equation (51) for a unit-volume we obtain:

$$\rho_s \cdot v_s \frac{dv_s}{ds} = \rho_L \cdot v_L \frac{dv_L}{ds} - C_R \frac{1}{2} \rho_L (v_s - v_L)^2 \quad (52)$$

The differential equation was solved numerically by a step method. The steps used are $ds = 0.025$ m. At the Venturi entrance the solid-phase velocity v_s is assumed equal to the liquid-phase velocity v_L . The liquid velocity v_L can be calculated for each cross section in the Venturi. Since the value C_R is not known it has to be assumed. This assumed C_R value will lead to the first approximation. The step method will give local values of v_s and so the local relative velocity $(v_s - v_L)$ can be computed. Furthermore, the average of the relative velocity $\overline{(v_s - v_L)}$ is obtained and the average change of the relative velocity $\Delta \overline{(v_s - v_L)}$. We shall now compare the assumed resistance coefficient C_R with the experimental results. Equation (46) correlated the drag with the loss due to concentration and reads

$$(b - b_0) = \frac{\text{Drag}}{A \cdot \gamma} \quad (46)$$

Combining known equation (46) and equation (41) we get:

$$1.95 \cdot l_v \cdot c = \frac{\text{Drag}}{A \cdot \gamma} \quad (53)$$

For the drag equation we use the same equation as used in the differential equation and obtain

$$1.95 \cdot l_v = \frac{(\overline{v_s - v_L})^2}{2g} \cdot C_R \quad (54)$$

Introducing $(\overline{v_s - v_L})$ as calculated with an assumed C_R value in the first approximation, we are able to determine the assumption was satisfactory. If the assumed C_R value is satisfactory, it will be taken for further considerations, if it was not we have to keep on trying, till we find a sufficiently satisfactory C_R - value.

This procedure of solving equation (52) and comparing it with experimental values was done, due to its elaborate procedure for the two extreme velocities in our investigation only. As a minimum velocity 2m/s was taken and 4 m/s was the maximum velocity. In Fig. V-6 the velocity histogram is plotted for the extreme velocities and for both the solid and liquid velocity. It was found that the solid phase has a smaller velocity at the throat of the venturi and will reach its maximum after passing the throat. This can easily be seen in the case of the 2 m/sec velocity, but is not so apparent in the case of 4 m/sec, since the chosen ds was probably too big to show this effect. But with both velocities it can be seen that, when the particles leave the Venturi meter their velocity is larger than that of the liquid.

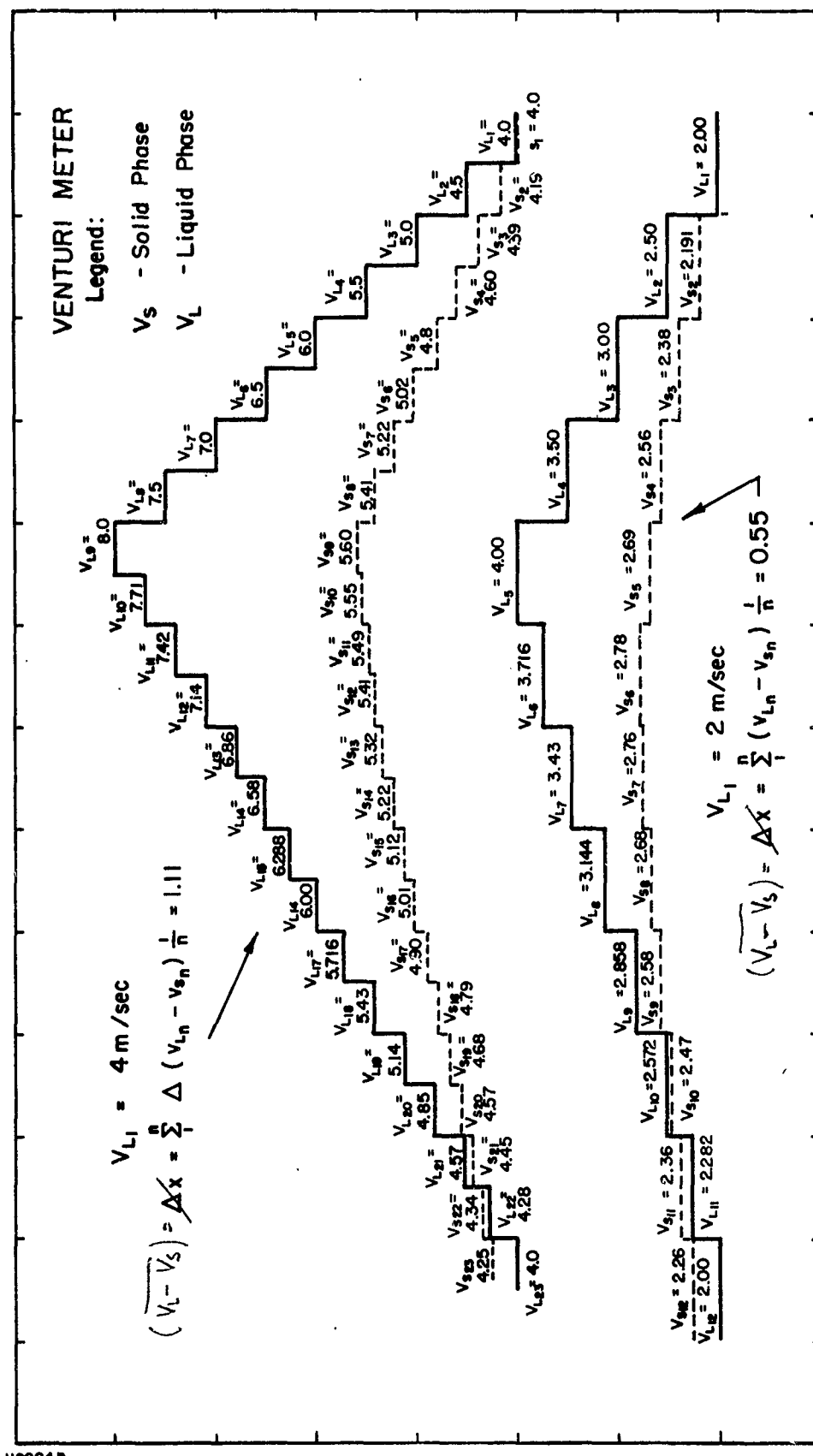


FIGURE V-6 - VELOCITY HISTOGRAM FOR LIQUID AND SOLID PHASE

H9004 B

The results of the first and last approximation for both extreme velocities are summarized in Table V-1.

In Fig. V-7 the data are plotted on a graph of Reynolds number versus drag coefficient. In the same graph the steady state drag coefficients of a sphere, a cylinder, and a disk are plotted (Ref. 12). By comparing our data with the steady state drag coefficients, we notice that our drag coefficients are consistently higher. Also on the same graph are shown drag coefficients obtained with objects being accelerated, which indicate the same trend. The research carried out by Bugliarello (Ref. 5) on spheres showed a very similar effect, i.e. at his low Reynolds numbers he obtained resistance coefficients beyond $C_R = 10$. Torobin & Gauvin (Ref. 6) who computed the acceleration parameter for Bugliarello's results, found a variation of this parameter from 0.01 to 0.4. Bugliarello's results are shown on Fig. V-7. Laird et al. (Ref. 7) obtained their data with a decelerating cylinder and observed also this effect, that the drag coefficient was enlarged. Keim (Ref. 8) did his work with an accelerated cylinder; his data were examined for the acceleration parameters by Torobin & Gauvin (Ref. 6) and are shown in Fig. V-7. The data indicated, that an increase in the acceleration parameter is proportional to an increase in the resistance coefficient. The same phenomenon can be seen in the present results. The phenomenon just described was also noticed by Lumon (Ref. 3 and Ref. 4).

The research of all the references was apparently carried out

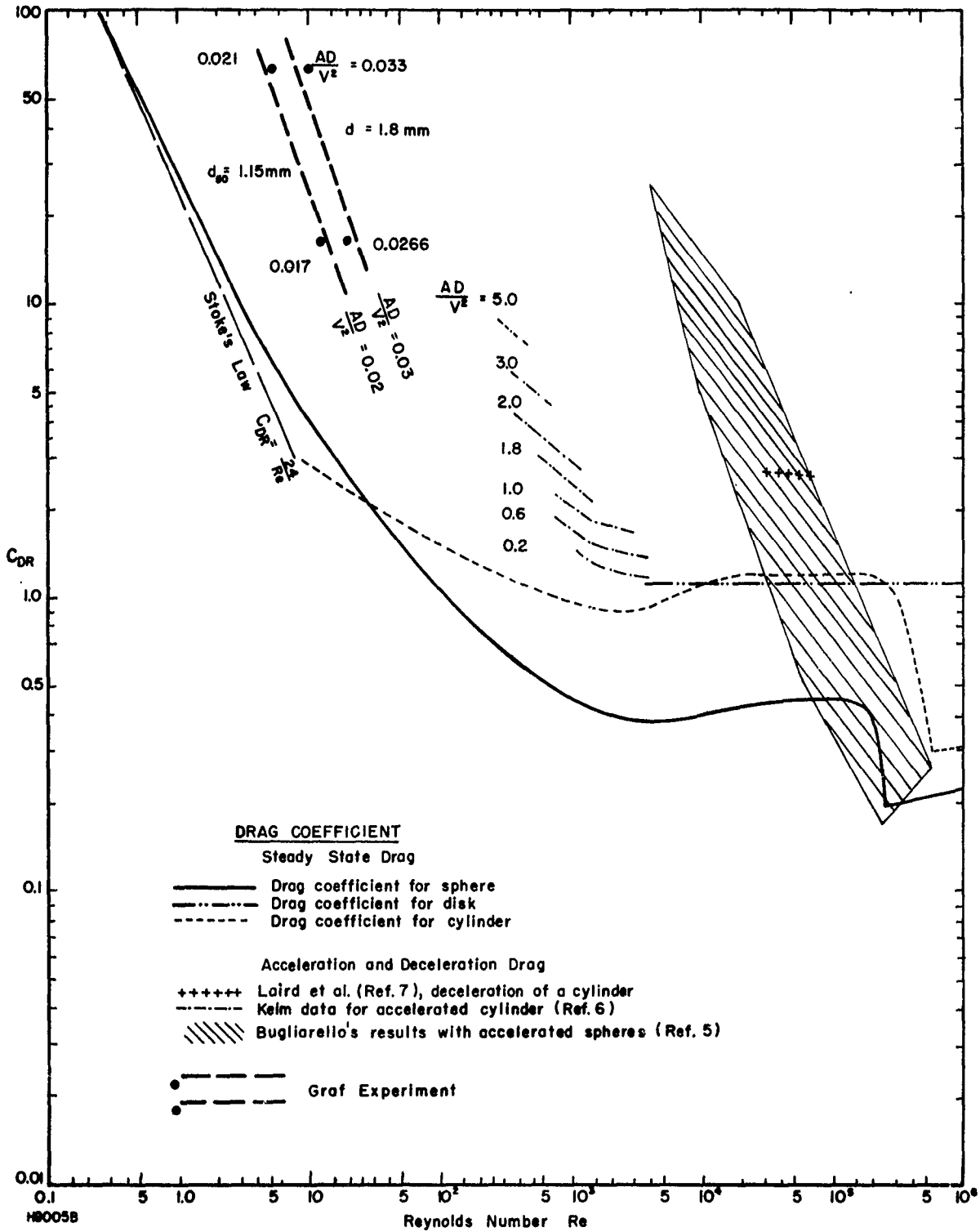


FIGURE V-7- DRAG COEFFICIENT

in free stream velocity. In the present work a free stream vorticity exists. A paper dealing with the "Effects of fluid turbulence on particle drag-coefficient" by Torobin and Gauvin (Ref. 9) reports a shift of the laminar-turbulent boundary layer transition due to free stream velocity. Yet Ref. 9 does not show in his graph an observed deviation at other Reynolds numbers than the one where the transition takes place. Depending on the intensity of the turbulence the transition is between Reynolds number 10^3 and 10^4 . Furthermore, all of the investigations conducted by the various investigators were with smooth objects. Though it can be said that the roughness will be submerged, at these Reynolds numbers, in the present tests in the laminar layer in the case of steady state, there exists no information if this is also true in an unsteady case.

2.2.3 Acceleration Drag. We have already mentioned that the drag equation used in part 2.2.2 of this chapter should be used where the acceleration effects are of minor importance. With C_R 10 times that of uniform motion the acceleration term appears to be predominant and equation (49) for the drag is a poor choice. Equation (48) would be much better. In equation (48) U_p is replaced by $(v_s - v_L)$ and we have:

$$\text{Drag}_2 = K_1 (v_s - v_L)^2 + k \cdot V_s \cdot \rho_L (\dot{v}_s - \dot{v}_L) \quad (48)$$

In Fig. V-8 it is shown that at each cross section in the Venturi meter, the value of the ratio $\frac{(v_s - v_L)^2}{(\dot{v}_s - \dot{v}_L)}$ is about the same. This means that an increase of the second term in equation (48) will cause a proportional increase in the first term. We shall now write equation (48) for an average drag over the length of the Venturi meter. Then we get:

$$\text{Drag}_2 = K_1 (\overline{v_S - v_L})^2 + k (V_S \cdot \rho_L) (\overline{v_S - v_L}) \quad (55)$$

We shall combine equation (55) with equation (53) and have

$$(1.95 \cdot l_v) \cdot c = (K_1 \frac{(\overline{v_S - v_L})^2}{A \cdot \gamma} + k (V_S \cdot \rho_L) \frac{\overline{v_S - v_L}}{A \cdot \gamma}) \cdot c \quad (56)$$

In equation (56) the coefficient K_1 is replaced by $\frac{1}{2} C_{DR} \cdot \rho_L A$ and divided by the concentration c . Writing now this equation for unit volume we get:

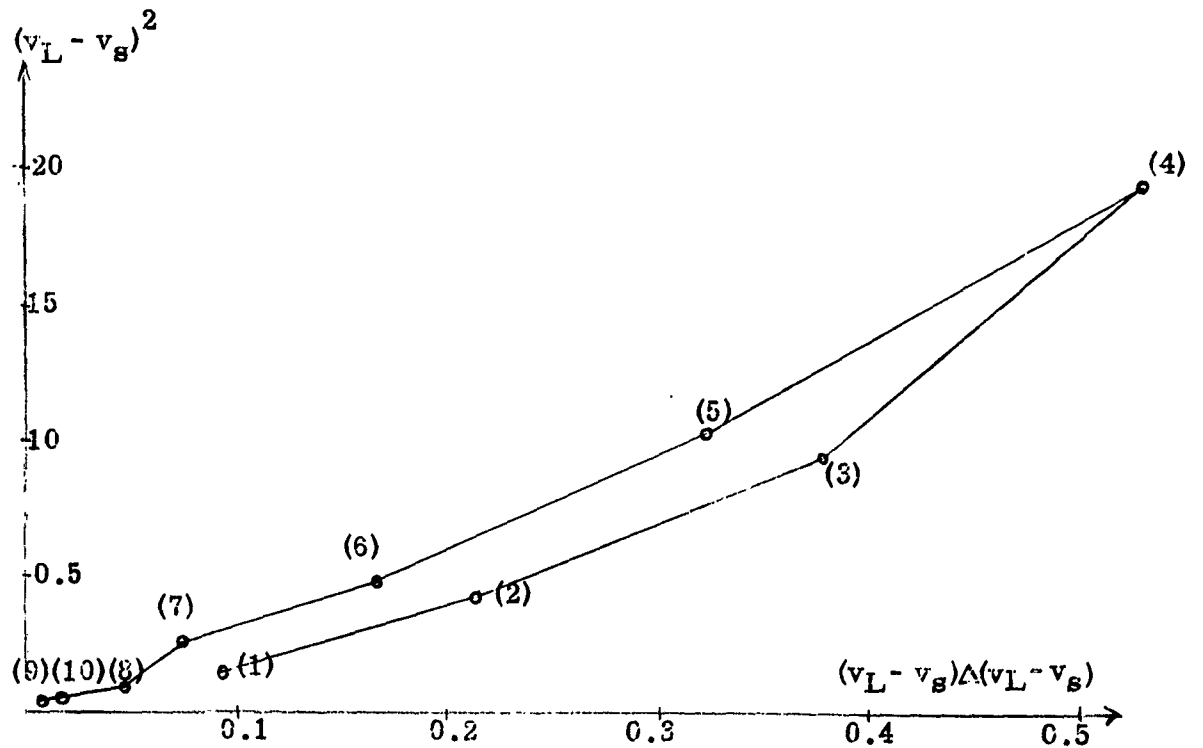
$$1.95 \cdot l_v = C_{DR} \frac{(\overline{v_S - v_L})^2}{2g} + k \frac{1}{g} (\overline{v_S - v_L}) \quad (57)$$

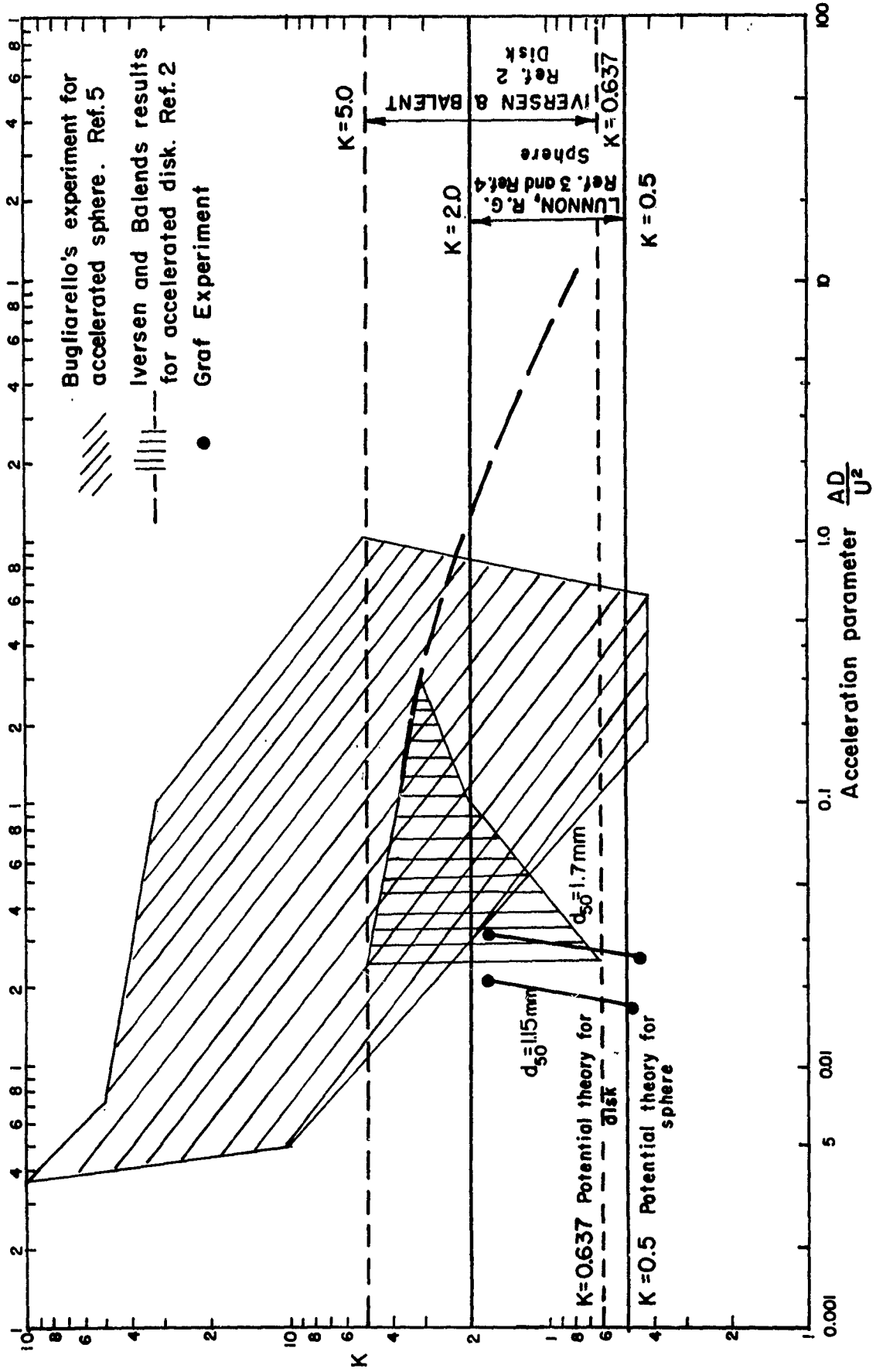
$(\overline{v_S - v_L})$ and $\Delta (\overline{v_S - v_L})$ have been determined in part 2.2.2 of this chapter and are tabulated in ^{Tab. V-1} Fig. V-8. From the same table the Reynolds number can be obtained and with a given Reynolds number the drag coefficient C_{DR} can be obtained from graph Fig. V-7. The term on the left side of equation (57) is an experimental constant, already discussed and g is the acceleration due to gravity. Everything is known in equation (57) and it can be solved for k , the added mass coefficient. The added mass coefficient was computed for both extreme velocities and the two different grain sizes and is tabulated in table V-1. It was mentioned in part 2.2.1 of this chapter, that the added mass coefficient could be correlated with a dimensionless acceleration parameter. Iversen and Balent (Ref. 2) were able to find a satisfactory correlation for their data, especially at high acceleration parameters. Lunnon (Ref. 3 and Ref. 4) reported to have obtained values of k ranging from 0.5 to 2.0. Bugliarello (Ref. 5) failed to give a satisfactory correlation, neither did his values correlate with $\frac{AD}{v^2}$, nor were they in the range reported by Lunnon. The two last authors investigated a sphere, while

Fig. V - 8

Check for Proportionality of $(v_L - v_S)^2$ and $(v_L - v_S)$ done for
 $v_L = 2\text{m/sek}$ and Sand No. 2

| | v_L | v_S | $v_L - v_S$ | $(v_L - v_S)^2$ | $\Delta(v_L - v_S)$ | $(v_L - v_S)(\Delta(v_L - v_S))$ | |
|-------|-------|-------|-------------|-----------------|---------------------|----------------------------------|------|
| v_1 | 2.00 | 2.00 | 0.00 | | 0.31 | 0.00 | |
| 2 | 2.50 | 2.19 | 0.31 | 0.09 | 0.31 | 0.09 | (1) |
| 3 | 3.00 | 2.38 | 0.62 | 0.38 | 0.34 | 0.21 | (2) |
| 4 | 3.50 | 2.54 | 0.96 | 0.92 | 0.42 | 0.38 | (3) |
| 5 | 4.00 | 2.62 | 1.38 | 1.90 | 0.38 | 0.52 | (4) |
| 6 | 3.71 | 2.72 | 1.00 | 1.00 | 0.32 | 0.32 | (5) |
| 7 | 3.43 | 2.75 | 0.68 | 0.46 | 0.24 | 0.16 | (6) |
| 8 | 3.14 | 2.70 | 0.44 | 0.19 | 0.19 | 0.084 | (7) |
| 9 | 2.86 | 2.61 | 0.25 | 0.062 | 0.18 | 0.045 | (8) |
| 10 | 2.57 | 2.50 | 0.07 | 0.005 | 0.05 | 0.004 | (9) |
| 11 | 2.28 | 2.30 | 0.12 | 0.014 | 0.17 | 0.02 | (10) |
| 12 | 2.00 | 2.29 | 0.29 | 0.080 | | | (11) |





H9008A

FIGURE V-9 - VIRTUAL MASS COEFFICIENT

Iversen and Balent did their work on a disk. In Fig. V-9 the authors' data are compared with the references just discussed. One might see that our data fall at least in a reasonable range (0.45 - k - 1.70). Since our scope was not to investigate the validity of the added mass coefficient, nor its dependence from the acceleration parameter, the number of values obtained is limited. The particle grain size range and the velocity range were just too small. All we can conclude is that the magnitude of the added mass coefficient is reasonable and provided probably a possible explanation of the high drag or the large energy loss .

Sand No. 2 $d_{50} = 1.15 \times 10^{-3} \text{ m}$

| $v_L = 2 \text{ m/s}$ | CR | CR' | $(v_s - v_L)$ | $\Delta(v_s - v_L)$ | ΔS | $N_R = \frac{(v_s - v_L) d_{50}}{v}$ | $\frac{AD}{v^2} = \frac{\Delta(v_s - v_L) d_{50}}{\Delta S (v_s - v_L)}$ | $\frac{R}{X}$ |
|-----------------------|------|------|---------------|---------------------|------------|--------------------------------------|--|---------------|
| 1. Approx. | 1 | 43.5 | 0.66 | 0.19 | 0.0254 | -- | -- | -- |
| 2. Approx. | 83 | 63.0 | 0.55 | 0.25 | 0.0254 | 6.3 | 0.021 | 1.67 |
| $v_L = 4 \text{ m/s}$ | | | | | | | | |
| 1. Approx. | 1 | 30.8 | 1.14 | 0.20 | 0.0127 | -- | -- | -- |
| 2. Approx. | 20.5 | 16.2 | 1.11 | 0.21 | 0.0127 | 12.7 | 0.017 | 0.47 |

Sand No. II $d_{50} = 1.7 \times 10^{-3} \text{ m}$

| | | | | | | | | |
|-----------------------|------|------|------|------|--------|------|--------|------|
| $v_L = 2 \text{ m/s}$ | | | | | | | | |
| | 86 | 63.0 | 0.55 | 0.25 | 0.0254 | 99 | 0.033 | 1.70 |
| $v_L = 4 \text{ m/s}$ | | | | | | | | |
| | 21.0 | 16.2 | 1.11 | 0.21 | 0.0127 | 19.8 | 0.0206 | 0.45 |

Table V-1

VI. SUMMARY, CONCLUSIONS, AND SUGGESTIONS

The investigation described in this report was concerned with two-phase flow in a closed pipe system.

A device which gives information on flow rate of mixture and the concentration was designed, tested, and found useful. This device, called a "Loop", consists of two vertical pipes, with opposite flow directions. Combination (the summation and the difference) of the two head readings for each flow gave us the desired results. The effect was explained by a theory.

Furthermore, a Venturi meter was tested for its applicability in a two-phase flow. Besides the usually recorded pressure drop, the pressure loss across the horizontal Venturi meter was obtained. It is shown by experiment and theory, that the pressure readings in terms of mixture gives information of the flow rate. The energy loss was correlated with the concentration. An attempt was made to explain also this by a theory. Since the concept of virtual mass seems to be important, and the existing literature is quite incomplete, our explanation is of limited value.

For all practical purposes it can be stated that the "Loop" system will provide a possibility to determine immediately the flow rate of mixture and the concentration, if two manometer readings one at a riser section and one on downcomer section are known. The practical application of the modified Venturi meter is not quite as straight forward.

In order to determine the concentration the flow rate must be known, but in order to obtain the flow rate, the concentration has to be known. But fast trial and error solution will lead to a reliable determination of flow rate and concentration.

The two-phase flow problem requires additional research. In a rather extensive way straight pipe tests were already investigated. But not too much has been done in studying different units in pipeline systems, their applicabilities and their effects. The present study was concerned with a flow meter, the Venturi tube in a horizontal position. An immediate suggestion could be to investigate this same flow meter in vertical or oblique pipe systems. Also it would be of interest to study the behavior of other flow meters like the orifice meter, metering nozzle and elbow meters, in a sand-water mixture.

It is suggested therefore that a study with sand of different geometry and density would make it possible to establish more general constants. It is believed that the pipe diameter will not change the results, although no attempt was made to check this.

The results obtained at the Venturi meter can probably be plotted in form of a nomograph, which would provide a fast interpretation of the Venturi meter reading.

VII. ACKNOWLEDGEMENT

The author gratefully acknowledges the extensive guidance and help received during the course of this investigation from Professor H. A. Einstein. Appreciation also is expressed to K. Bermel, W. A. Hewitt and W. J. Ferguson for their cooperation and help with the design and construction of the experimental equipment.

VIII. NOMENCLATURE

| SYMBOL | EXPLANATION |
|--------------------|--|
| A | Area |
| A ₁ | Area of pipe cross section |
| A ₂ | Area of cross section at throat of Venturi-meter |
| a _m | Pressure drop in terms of mixture |
| $\frac{AD}{V^2}$ | Acceleration modulus: $\frac{\text{Acceleration} \times \text{Length}}{(\text{Velocity})^2}$ |
| b | total energy loss across Venturi meter |
| b - b ₀ | energy loss across Venturi meter, due to concentration |
| c _D | concentration in downcomer section |
| c _R | concentration in riser section |
| c | average concentration in volume percentage; taken up by solid phase |
| (1-c) | average concentration in volume percentage; taken up by liquid phase. |
| C _{DR} | steady state drag coefficient |
| C _R | resistance coefficient, dependent on steady state and unsteady state effects |
| C _v | coefficient in flow rate equation of Venturi meter, taking care of real fluid effects |
| d ₅₀ | average grain size diameter |
| ds | or Δs stepwise increment in differ |
| Drag ₁ | steady state drag |
| Drag ₂ | summation of steady state and unsteady state drag |

| SYMBOL | EXPLANATION |
|---------------------|---|
| Drag ₃ | combined steady state and unsteady state drag |
| F | force |
| F _{fr} | wall friction force |
| F _p | particle force |
| g | acceleation due to gravity |
| L | length of riser and downcomer section |
| l _v | length over which energy loss at Venturi meter is recorded |
| k | added or virtual mass coefficient |
| K ₁ | steady state constant, including C _{DR} |
| K ₃ | steady and unsteady state constant |
| m | symbol for mass |
| Q | or Q _m flow rate of mixture; Q = Q _s + Q _L |
| Q _s | flow rate of solid phase |
| Q _L | flow rate of liquid phase |
| R _D | manometer reading at downcomer section |
| R _R | manometer reading at riser section |
| R _{fr} | manometer reading due to friction |
| R _{susp} | manometer reading due to suspension |
| U _p | relative velocity of liquid and solid phase (V _p) |
| V _s | volume of solid particle |
| v or v _m | or velocity of mixture, m = Q/A |
| v _s | velocity of solid phase |
| v _L | velocity of liquid phase |

| SYMBOL | EXPLANATION |
|--------------------|---|
| v_{settl} | settling velocity |
| α | ratio of flow rate of solids to flow rate of mixture |
| $1 - \alpha$ | ratio of flow rate of liquids to flow rate of mixture |
| γ_L | specific weight of liquid phase |
| γ_s | specific weight of solid phase |
| γ_m | specific weight of mixture |
| ρ_L | density of liquid phase |
| ρ_s | density of solid phase |
| ρ_m | density of mixture |

IX. REFERENCES

- Ref. 1 Einstein, H. A. & Iversen, H. W., Jet pump model test for Pacific Coast Engineering Company, UCB, Eng., 6428, Iss. 1, Jan. 1960, (unpublished).
- Ref. 2 Iversen, H. W. & Balent, R., A correlating modulus for fluid resistance in accelerated motion, Journ. of Appl. Physics, Vol. 22, No. 3, pp 324-328, March, 1951.
- Ref. 3 Lunnon, R. G., Resistance of air to falling spheres, Phil. Mag., 6th Series, 47, 1924, p. 173.
- Ref. 4 Lunnon, R. G., Fluid resistance to moving spheres, Proc. Roy. Soc. of London, Series A, 1926, p. 302.
- Ref. 5 Bugliarello, G., La resistenza al moto accelerato di sfera in acqua, "La Ricerca Scientifica", Anno 26°-N. 2, Feb. 1956.
- Ref. 6 Torobin, L. B. & W. H. Gauvin, Fundamental aspects of solids-gas flow, Part III, Canadian Journ. of Chem. Eng. 37, pp 224-236, Dec. 1959.
- Ref. 7 Laird, A. D. K., C. A. Johnson & R. W. Walker, Water forces on accelerated cylinders, Journ. of Waterways & Harbors Div., ASCE, Vol. 85, No. WW1, March 1959.
- Ref. 8 Keim, S. R., Fluid resistance to cylinders in accelerated motion, Journ. of Hydraulics Div. ASCE, Vol. 82, HY6, Dec. 1956.
- Ref. 9 Torobin, L. B. & W. H. Gauvin, Fundamental aspects of solid-gas flow, Part V, Canadian Journ. of Chem. Eng. 38, pp 189-200, Dec. 1960.
- Ref. 10 Prandtl, L. & O. Tietjens, Applied hydro- and aeromechanic, Dover Publications, Inc., 1934 (Transl. by Den Hartog).
- Ref. 11 Bessel, F. W., On the incorrectness of the reduction to a vacuum formerly used in Pendulum Experiments, Berlin Academy, 1826.
- Ref. 12 Vennard, J. K., "Elementary Fluid Mechanics" 4th edition, John Wiley & Sons, Inc.

X. APPENDIX

Appendix 1. Summary of Data on Loop System

Summary of Data

Loop System

| 1 | 2 | 3 | 4 | 5 | 6 | 7 | 8 |
|-----------|------------------------|------|--------------------|-----------|-------|--------|---------------|
| flow rate | sum. γ mixt. | sum. | Manometer Readings | | diff. | conc. | no. |
| L/sec | m | m | riser | downcomer | m | vol. % | series run |
| - | - | 4+5 | - | - | 4-5 | - | - |

Clear Water

| | | | | | | | |
|--------|-------|-------|-------|-------|---|---|----|
| 10.00* | 0.142 | 0.142 | 0.071 | 0.071 | 0 | 0 | 19 |
| 10.55* | 0.152 | 0.152 | 0.076 | 0.076 | 0 | 0 | 20 |
| 12.10* | 0.214 | 0.214 | 0.107 | 0.107 | 0 | 0 | 30 |
| 13.82* | 0.292 | 0.292 | 0.146 | 0.146 | 0 | 0 | 40 |
| 15.00* | 0.348 | 0.348 | 0.175 | 0.173 | 0 | 0 | 50 |
| 16.55* | 0.388 | 0.388 | 0.194 | 0.194 | 0 | 0 | 60 |

* An average over a number of measurements is recorded.

Sand No. 2

| | | | | | | | |
|-------|-------|-------|-------|--------|-------|------|-------|
| 7.7 | 0.113 | 0.143 | 0.338 | -0.195 | 0.533 | 16.5 | 19-1 |
| 8.6 | 0.125 | 0.140 | 0.323 | -0.183 | 0.406 | 8. | 2 |
| 8.4 | 0.122 | 0.144 | 0.318 | -0.174 | 0.492 | 11.4 | 3 |
| 9.8 | 0.137 | 0.140 | 0.305 | -0.165 | 0.470 | 3.8 | 4 |
| 8.8 | 0.116 | 0.138 | 0.290 | -0.152 | 0.442 | 11.0 | 5 |
| 9.1 | 0.125 | 0.143 | 0.268 | -0.125 | 0.393 | 8.5 | 6 |
| 9.1 | 0.125 | 0.144 | 0.244 | -0.100 | 0.344 | 8.5 | 7 |
| 9.7 | 0.131 | 0.147 | 0.223 | -0.076 | 0.299 | 6.1 | 8 |
| 9.4 | 0.131 | 0.143 | 0.201 | -0.058 | 0.259 | 5.3 | 9 |
| 8.9 | 0.128 | 0.143 | 0.177 | -0.034 | 0.201 | 6.2 | 10 |
| 9.35 | 0.131 | 0.140 | 0.155 | -0.015 | 0.170 | 4.5 | 11 |
| 9.70 | 0.125 | 0.131 | 0.137 | -0.006 | 0.143 | 3.4 | 12 |
| 10.5 | 0.125 | 0.128 | 0.122 | +0.006 | 0.116 | 1.3 | 13 |
| 9.4 | 0.125 | 0.131 | 0.113 | +0.018 | 0.095 | 2.4 | 14 |
| 9.80 | 0.128 | 0.134 | 0.107 | +0.027 | 0.080 | 2.3 | 15 |
| 10.05 | 0.131 | 0.131 | 0.098 | +0.033 | 0.065 | 0.9 | 16 |
| 10.7 | 0.131 | 0.131 | 0.091 | +0.040 | 0.051 | 0.8 | 17 |
| 8.5 | 0.119 | 0.140 | 0.280 | -0.140 | 0.420 | 10.8 | 19-18 |
| 9.3 | 0.122 | 0.137 | 0.259 | -0.122 | 0.381 | 7.4 | 19 |
| 9.7 | 0.125 | 0.140 | 0.241 | -0.101 | 0.342 | 7.0 | 20 |
| 9.2 | 0.128 | 0.144 | 0.223 | -0.079 | 0.302 | 8.4 | 21 |
| 9.4 | 0.131 | 0.143 | 0.207 | -0.064 | 0.271 | 5.4 | 22 |
| 9.3 | 0.125 | 0.131 | 0.183 | -0.052 | 0.235 | 3.5 | 23 |
| 9.9 | 0.122 | 0.132 | 0.162 | -0.030 | 0.192 | 4.2 | 24 |
| 9.9 | 0.125 | 0.135 | 0.147 | -0.012 | 0.159 | 3.7 | 25 |

Summary of Data

Loop System

| 1 | 2 | 3 | 4 | 5 | 6 | 7 | 8 |
|------------|-------------------------------|-------|--|--------|-------|--------|---------------|
| flow rate | <u>sum.</u> γ mixt. | sum. | <u>Manometer Readings</u> riser downcomer | | diff. | conc. | no. |
| L/sec | m | m | m | m | m | vol. % | series run |
| - | - | 4+5 | - | - | 4-5 | - | - |
| Sand No. 2 | | | | | | | |
| 9.3 | 0.122 | 0.131 | 0.134 | -0.003 | 0.137 | 4.4 | 19-26 |
| 9.5 | 0.128 | 0.134 | 0.125 | +0.009 | 0.116 | 1.9 | 27 |
| 9.5 | 0.128 | 0.134 | 0.116 | +0.018 | 0.098 | 3.3 | 28 |
| 10.45 | 0.128 | 0.134 | 0.167 | +0.027 | 0.080 | 1.0 | 29 |
| 8.45 | 0.119 | 0.150 | 0.304 | -0.154 | 0.458 | 11.4 | 19-30 |
| 9.00 | 0.119 | 0.148 | 0.286 | -0.138 | 0.424 | 9.6 | 31 |
| 9.35 | 0.125 | 0.145 | 0.263 | -0.118 | 0.381 | 6.4 | 32 |
| 8.60 | 0.119 | 0.141 | 0.244 | -0.103 | 0.347 | 9.0 | 33 |
| 9.60 | 0.125 | 0.140 | 0.226 | -0.086 | 0.302 | 4.8 | 34 |
| 9.10 | 0.128 | 0.146 | 0.207 | -0.061 | 0.268 | 6.0 | 35 |
| 9.4 | 0.131 | 0.148 | 0.194 | -0.046 | 0.240 | 4.9 | 36 |
| 10.00 | 0.131 | 0.142 | 0.172 | -0.030 | 0.202 | 2.7 | 37 |
| 9.7 | 0.131 | 0.147 | 0.157 | -0.015 | 0.172 | 3.3 | 38 |
| 9.9 | 0.134 | 0.140 | 0.147 | -0.003 | 0.150 | 3.3 | 39 |
| 10.45 | 0.134 | 0.145 | 0.135 | +0.010 | 0.125 | 3.1 | 40 |
| 9.9 | 0.137 | 0.146 | 0.125 | +0.021 | 0.104 | 2.8 | 41 |
| 9.8 | 0.137 | 0.143 | 0.113 | +0.030 | 0.083 | 1.4 | 42 |
| 10.45 | 0.137 | 0.143 | 0.104 | +0.039 | 0.065 | 1.3 | 43 |
| 10.40 | 0.137 | 0.143 | 0.097 | +0.046 | 0.051 | 0.9 | 44 |
| 10.00 | 0.134 | 0.137 | 0.091 | +0.046 | 0.045 | 0.5 | 45 |
| 9.80 | 0.134 | 0.136 | 0.088 | +0.048 | 0.040 | 0.9 | 46 |
| 7.0 | 0.098 | 0.132 | 0.360 | -0.228 | 0.588 | 17.6 | 19.47 |
| 8.05 | 0.107 | 0.139 | 0.358 | -0.219 | 0.577 | 14.2 | 48 |
| 8.4 | 0.122 | 0.148 | 0.352 | -0.204 | 0.556 | 9.2 | 49 |
| 8.4 | 0.119 | 0.150 | 0.339 | -0.189 | 0.528 | 10.4 | 50 |
| 8.7 | 0.125 | 0.156 | 0.326 | -0.170 | 0.496 | 10.5 | 51 |
| 9.5 | 0.131 | 0.156 | 0.308 | -0.152 | 0.452 | 7.7 | 52 |
| 9.3 | 0.125 | 0.151 | 0.282 | -0.131 | 0.413 | 9.3 | 53 |
| 8.8 | 0.125 | 0.150 | 0.260 | -0.110 | 0.370 | 9.3 | 54 |
| 9.4 | 0.125 | 0.145 | 0.242 | -0.097 | 0.339 | 6.2 | 55 |
| 9.6 | 0.125 | 0.144 | 0.220 | -0.076 | 0.396 | 6.2 | 56 |
| 9.3 | 0.131 | 0.146 | 0.201 | -0.055 | 0.256 | 3.9 | 57 |
| 10.1 | 0.131 | 0.142 | 0.188 | -0.046 | 0.234 | 2.7 | 58 |
| 10.4 | 0.128 | 0.143 | 0.173 | -0.030 | 0.203 | 4.0 | 59 |
| 10.4 | 0.134 | 0.145 | 0.160 | -0.015 | 0.175 | 3.1 | 60 |
| 10.1 | 0.134 | 0.145 | 0.151 | -0.006 | 0.157 | 2.2 | 61 |

Summary of Data

Loop System

| 1 | 2 | 3 | 4 | 5 | 6 | 7 | 8 |
|-----------|------------------------|------|--------------------|-----------|-------|--------|---------------|
| flow rate | <u>sum.</u> γ mixt. | sum. | Manometer Readings | | diff. | conc. | no. |
| L/sec | m | m | riser | downcomer | m | vol. % | series run |
| - | - | 4+5 | - | - | 4-5 | - | - |

Sand No. 2

| | | | | | | | |
|------|-------|-------|-------|--------|-------|------|-------|
| 11.6 | 0.140 | 0.144 | 0.138 | +0.006 | 0.132 | 0.8 | 19-62 |
| 9.7 | 0.131 | 0.141 | 0.126 | +0.015 | 0.111 | 2.8 | 63 |
| 9.8 | 0.137 | 0.140 | 0.116 | +0.024 | 0.092 | 0.9 | 64 |
| 9.7 | 0.134 | 0.143 | 0.113 | +0.030 | 0.083 | 2.8 | 65 |
| 9.9 | 0.140 | 0.147 | 0.107 | +0.040 | 0.067 | 0.5 | 66 |
| 10.6 | 0.140 | 0.140 | 0.094 | +0.046 | 0.048 | 0.9 | 67 |
| 10.0 | 0.137 | 0.137 | 0.088 | +0.049 | 0.039 | 0.5 | 68 |
| 10.4 | 0.134 | 0.137 | 0.085 | +0.052 | 0.032 | 0.5 | 69 |
| 8.2 | 0.155 | 0.204 | 0.430 | -0.226 | 0.656 | 1.8 | 30-1 |
| 8.5 | 0.155 | 0.205 | 0.404 | -0.199 | 0.603 | 1.9 | 2 |
| 10.2 | 0.189 | 0.206 | 0.386 | -0.180 | 0.566 | 6.7 | 3 |
| 9.6 | 0.163 | 0.208 | 0.367 | -0.159 | 0.526 | 17.5 | 4 |
| 10.3 | 0.180 | 0.214 | 0.345 | -0.131 | 0.476 | 11.9 | 5 |

Summary of Data

Loop System

| 1 | 2 | 3 | 4 | 5 | 6 | 7 | 8 |
|------------|------------------------|-------|--|--------|-------|-------|---------------|
| flow rate | <u>sum.</u> γ mixt. | sum. | <u>Manometer Readings</u> riser downcomer | | diff. | conc. | no. |
| L/sec | m | m | m | m | m | vol % | series run |
| - | - | - | 4+5 | - | 4-5 | - | - |
| Sand No. 2 | | | | | | | |
| 11.2 | 0.189 | 0.217 | 0.318 | -0.101 | 0.419 | 8.9 | 30-6 |
| 10.15 | 0.186 | 0.217 | 0.294 | -0.077 | 0.371 | 10.3 | 7 |
| 10.8 | 0.165 | 0.212 | 0.266 | -0.058 | 0.324 | 4.2 | 8 |
| 10.5 | 0.189 | 0.210 | 0.238 | -0.028 | 0.266 | 7.3 | 9 |
| 11.7 | 0.204 | 0.214 | 0.214 | -0.000 | 0.214 | 2.3 | 10 |
| 11.3 | 0.210 | 0.220 | 0.199 | +0.021 | 0.178 | 2.4 | 11 |
| 11.7 | 0.204 | 0.221 | 0.183 | +0.038 | 0.145 | 5.1 | 12 |
| 12.0 | 0.204 | 0.214 | 0.162 | +0.052 | 0.110 | 2.7 | 13 |
| 12.6 | 0.205 | 0.217 | 0.150 | +0.067 | 0.083 | 3.3 | 14 |
| 12.4 | 0.210 | 0.214 | 0.138 | +0.076 | 0.062 | 1.5 | 15 |
| 10.4 | 0.207 | 0.213 | 0.134 | +0.079 | 0.055 | 2.2 | 16 |
| 11.5 | 0.204 | 0.207 | 0.128 | +0.079 | 0.049 | 1.2 | 17 |
| 12.5 | 0.204 | 0.207 | 0.122 | +0.085 | 0.037 | 0.7 | 18 |
| 8.5 | 0.159 | 0.197 | 0.425 | -0.228 | 0.653 | 14.3 | 30-19 |
| 9.1 | 0.165 | 0.202 | 0.412 | -0.210 | 0.622 | 14.5 | 20 |
| 9.7 | 0.155 | 0.204 | 0.388 | -0.192 | 0.580 | 15.5 | 21 |
| 10.7 | 0.178 | 0.207 | 0.368 | -0.162 | 0.530 | 8.9 | 22 |
| 10.5 | 0.186 | 0.210 | 0.330 | -0.120 | 0.450 | 8.2 | 23 |
| 10.5 | 0.186 | 0.209 | 0.300 | -0.091 | 0.391 | 9.1 | 24 |
| 11.1 | 0.186 | 0.212 | 0.276 | -0.064 | 0.340 | 8.6 | 25 |
| 14.6 | 0.201 | 0.224 | 0.256 | -0.052 | 0.288 | 5.6 | 26 |
| 12.0 | 0.216 | 0.226 | 0.232 | -0.006 | 0.238 | 2.6 | 27 |
| 11.3 | 0.213 | 0.203 | 0.214 | +0.009 | 0.205 | 3.2 | 28 |
| 12.2 | 0.198 | 0.210 | 0.192 | +0.018 | 0.174 | 4.1 | 29 |
| 11.3 | 0.186 | 0.196 | 0.155 | +0.041 | 0.114 | 2.8 | 30 |
| 12.5 | 0.186 | 0.193 | 0.137 | +0.056 | 0.181 | 2.6 | 31 |
| 12.4 | 0.195 | 0.205 | 0.140 | +0.065 | 0.075 | 1.1 | 32 |
| 12.3 | 0.202 | 0.206 | 0.128 | +0.078 | 0.050 | 0.7 | 33 |
| 12.0 | 0.202 | 0.205 | 0.122 | +0.083 | 0.039 | 0.8 | 34 |
| 8.2 | 0.151 | 0.208 | 0.424 | -0.216 | 0.640 | 22.0 | 30-40 |
| 9.4 | 0.171 | 0.202 | 0.400 | -0.198 | 0.598 | 12.1 | 41 |
| 11.0 | 0.164 | 0.195 | 0.378 | -0.183 | 0.561 | 11.2 | 42 |
| 10.1 | 0.161 | 0.197 | 0.360 | -0.163 | 0.523 | 13.5 | 43 |
| 12.0 | 0.183 | 0.204 | 0.335 | -0.131 | 0.466 | 6.9 | 44 |
| 9.9 | 0.164 | 0.203 | 0.310 | -0.107 | 0.417 | 15.3 | 45 |
| 12.1 | 0.183 | 0.204 | 0.284 | -0.080 | 0.364 | 7.2 | 46 |
| 12.4 | 0.189 | 0.209 | 0.258 | -0.049 | 0.307 | 6.6 | 47 |
| 12.4 | 0.208 | 0.213 | 0.240 | -0.027 | 0.267 | 1.8 | 48 |
| 11.9 | 0.192 | 0.213 | 0.222 | -0.009 | 0.231 | 7.3 | 49 |

Summary of Data

Loop System

| 1 | 2 | 3 | 4 | 5 | 6 | 7 | 8 |
|-----------|------------------------|------|---------------------------|-----------|-------|--------|--------|
| flow rate | <u>sum.</u> γ mixt. | sum. | <u>Manometer Readings</u> | | diff. | conc. | no. |
| L/sec | m | m | riser | downcomer | m | vol. % | series |
| | | | m | m | | | run |
| - | - | - | 4+5 | - | 4-5 | - | - |

Sand No. 2

| | | | | | | | |
|------|-------|-------|-------|--------|-------|------|-------|
| 12.3 | 0.208 | 0.187 | 0.202 | +0.005 | 0.187 | 2.9 | 30-50 |
| 7.7 | 0.157 | 0.203 | 0.413 | -0.210 | 0.413 | 19.5 | 30-51 |
| 10.2 | 0.171 | 0.203 | 0.398 | -0.195 | 0.398 | 12.1 | 52 |
| 10.6 | 0.174 | 0.208 | 0.385 | -0.177 | 0.385 | 12.5 | 53 |
| 10.1 | 0.177 | 0.192 | 0.364 | -0.152 | 0.344 | 12.2 | 54 |
| 10.5 | 0.168 | 0.202 | 0.336 | -0.134 | 0.336 | 7.8 | 55 |
| 11.7 | 0.183 | 0.210 | 0.314 | -0.104 | 0.314 | 8.6 | 56 |
| 12.0 | 0.204 | 0.213 | 0.293 | -0.080 | 0.293 | 5.0 | 57 |
| 11.4 | 0.189 | 0.210 | 0.268 | -0.058 | 0.268 | 6.8 | 58 |
| 11.8 | 0.192 | 0.211 | 0.247 | -0.036 | 0.247 | 5.8 | 59 |
| 12.5 | 0.198 | 0.214 | 0.232 | -0.018 | 0.232 | 4.4 | 60 |
| 11.4 | 0.189 | 0.203 | 0.214 | -0.009 | 0.212 | 5.2 | 61 |
| 11.8 | 0.180 | 0.196 | 0.190 | +0.006 | 0.184 | 5.8 | 62 |
| 12.3 | 0.192 | 0.204 | 0.174 | +0.030 | 0.144 | 3.7 | 63 |
| 11.4 | 0.195 | 0.205 | 0.165 | +0.040 | 0.120 | 3.2 | 64 |
| 12.1 | 0.198 | 0.204 | 0.155 | +0.049 | 0.106 | 2.6 | 65 |
| 11.9 | 0.198 | 0.208 | 0.150 | +0.058 | 0.092 | 2.3 | 66 |
| 12.0 | 0.201 | 0.204 | 0.140 | +0.064 | 0.076 | 0.8 | 67 |
| 12.2 | 0.198 | 0.204 | 0.131 | +0.073 | 0.058 | 1.1 | 68 |
| 11.7 | 0.198 | 0.201 | 0.128 | +0.073 | 0.055 | 0.8 | 69 |
| 11.6 | 0.198 | 0.201 | 0.122 | +0.079 | 0.043 | 0.8 | 70 |
| 11.2 | 0.201 | 0.24 | 0.50 | -0.256 | 0.760 | 12.5 | 40-1 |
| 11.4 | 0.204 | 0.25 | 0.48 | -0.229 | 0.715 | 13.0 | 2 |
| 11.8 | 0.210 | 0.25 | 0.44 | -0.192 | 0.63 | 13.4 | 3 |
| 11.6 | 0.216 | 0.26 | 0.42 | -0.159 | 0.58 | 14.0 | 4 |
| 11.7 | 0.229 | 0.27 | 0.38 | -0.107 | 0.49 | 13.1 | 5 |
| 12.1 | 0.253 | 0.29 | 0.33 | -0.043 | 0.37 | 7.8 | 6 |
| 13.4 | 0.259 | 0.29 | 0.28 | +0.006 | 0.29 | 7.4 | 7 |
| 13.6 | 0.265 | 0.28 | 0.23 | +0.05 | 0.18 | 4.9 | 8 |
| 13.8 | 0.277 | 0.28 | 0.20 | +0.08 | 0.12 | 1.3 | 9 |
| 14.1 | 0.277 | 0.27 | 0.18 | +0.09 | 0.09 | 0.9 | 10 |
| 13.9 | 0.277 | 0.27 | 0.17 | +0.107 | 0.06 | 1.0 | 11 |
| 10.1 | 0.201 | 0.25 | 0.48 | -0.23 | 0.71 | 17.5 | 40-12 |
| 11.2 | 0.208 | 0.26 | 0.45 | -0.19 | 0.64 | 15.8 | 13 |
| - | - | - | 0.42 | -0.15 | 0.57 | 15.1 | 14 |
| 12.3 | 0.238 | 0.28 | 0.39 | -0.11 | 0.50 | 11.4 | 15 |
| 13.4 | 0.275 | 0.26 | 0.31 | 0.00 | 0.31 | 7.1 | 17 |
| 12.4 | 0.289 | 0.29 | 0.26 | +0.03 | 0.23 | 3.0 | 18 |

Summary of Data

Loop System

| 1 | 2 | 3 | 4 | 5 | 6 | 7 | 8 |
|-----------|------------------------|------|--------------------------|-----------|-------|--------|------------|
| flow rate | <u>sum.</u> γ mixt. | sum. | <u>Manometer Reading</u> | | diff. | conc. | no. |
| L./sec | m | m | riser | downcomer | m | vol. % | series run |
| - | - | - | 4+5 | - | 4-5 | - | - |

Sand No. 2

| | | | | | | | |
|------|-------|------|------|-------|------|------|-------|
| 13.4 | 0.259 | 0.28 | 0.21 | +0.07 | 0.14 | 4.10 | 40-19 |
| 13.7 | 0.275 | 0.28 | 0.18 | +0.10 | 0.08 | 1.30 | 20 |
| 13.8 | 0.268 | 0.28 | 0.17 | +0.11 | 0.06 | 1.70 | 21 |
| 14.2 | 0.275 | 0.27 | 0.16 | +0.11 | 0.04 | 0.60 | 22 |
| 14.0 | 0.278 | 0.27 | 0.15 | +0.12 | 0.03 | 0.96 | 23 |
| 14.0 | 0.278 | 0.28 | 0.15 | +0.13 | 0.02 | 0.30 | 24 |
| 10.2 | 0.217 | 0.28 | 0.42 | -0.14 | 0.56 | 16.0 | 40-25 |
| 12.0 | 0.228 | 0.28 | 0.39 | -0.11 | 0.50 | 12.5 | 26 |
| 12.5 | 0.240 | 0.27 | 0.34 | -0.07 | 0.41 | 9.6 | 27 |
| 11.7 | 0.253 | 0.29 | 0.31 | -0.02 | 0.33 | 6.1 | 28 |
| 12.7 | 0.292 | 0.31 | 0.29 | +0.02 | 0.27 | 2.5 | 29 |
| 10.4 | 0.210 | 0.28 | 0.45 | -0.17 | 0.62 | 17.6 | 40-30 |
| 13.0 | 0.222 | 0.27 | 0.43 | -0.16 | 0.59 | 12.3 | 31 |
| 12.3 | 0.226 | 0.28 | 0.40 | -0.12 | 0.52 | 13.0 | 32 |
| 12.5 | 0.243 | 0.29 | 0.36 | -0.07 | 0.43 | 9.5 | 33 |
| 12.9 | 0.258 | 0.28 | 0.32 | -0.04 | 0.36 | 5.7 | 34 |
| 12.4 | 0.254 | 0.29 | 0.29 | -0.00 | 0.29 | 8.8 | 35 |
| 14.6 | 0.268 | 0.29 | 0.25 | +0.04 | 0.21 | 5.0 | 36 |
| 11.3 | 0.222 | 0.28 | 0.42 | -0.14 | 0.54 | 13.7 | 40-37 |
| 12.7 | 0.228 | 0.27 | 0.38 | -0.11 | 0.49 | 10.4 | 38 |
| 12.6 | 0.250 | 0.25 | 0.30 | -0.05 | 0.35 | 6.8 | 40 |
| 13.5 | 0.256 | 0.25 | 0.27 | +0.02 | 0.25 | 7.5 | 41 |
| 13.6 | 0.265 | 0.29 | 0.24 | +0.05 | 0.19 | 5.4 | 42 |
| 13.1 | 0.271 | 0.28 | 0.22 | +0.06 | 0.16 | 1.05 | 43 |
| 11.8 | 0.226 | 0.26 | 0.37 | -0.11 | 0.48 | 12.0 | 40-44 |
| 13.0 | 0.235 | 0.27 | 0.32 | -0.05 | 0.37 | 8.8 | 45 |
| 13.4 | 0.253 | 0.27 | 0.29 | -0.02 | 0.31 | 5.1 | 46 |
| 13.1 | 0.253 | 0.27 | 0.27 | +0.00 | 0.27 | 3.8 | 47 |
| 12.5 | 0.259 | 0.28 | 0.26 | +0.02 | 0.24 | 4.4 | 48 |
| 12.5 | 0.268 | 0.28 | 0.24 | +0.04 | 0.20 | 2.8 | 49 |
| 13.8 | 0.256 | 0.28 | 0.21 | +0.07 | 0.14 | 4.2 | 50 |
| 13.8 | 0.263 | 0.27 | 0.18 | +0.09 | 0.09 | 1.7 | 51 |
| 13.1 | 0.263 | 0.27 | 0.17 | +0.10 | 0.07 | 1.7 | 52 |
| 12.8 | 0.256 | 0.32 | 0.47 | -0.15 | 0.62 | 16.4 | 50- 1 |
| 13.8 | 0.296 | 0.35 | 0.44 | -0.09 | 0.53 | 11.2 | 2 |
| 14.0 | 0.308 | 0.36 | 0.36 | -0.00 | 0.36 | 11.4 | 3 |
| 13.9 | 0.323 | 0.36 | 0.29 | +0.07 | 0.22 | 7.5 | 4 |
| 14.4 | 0.314 | 0.35 | 0.25 | +0.10 | 0.15 | 7.8 | 5 |

Summary of Data

Loop System

| 1 | 2 | 3 | 4 | 5 | 6 | 7 | 8 |
|-----------|-----------------|------|-------------------|-----------|-------|--------|--------|
| flow rate | sum. γ mixt. | sum. | Manometer Reading | | diff. | conc. | no. |
| L/sec | m | m | riser | downcomer | m | vol. % | series |
| | | | m | m | m | | run |
| - | - | - | 4+5 | - | 4-5 | - | - |

Sand No. 2

| | | | | | | | |
|------|-------|------|------|-------|------|------|-------|
| 13.5 | 0.336 | 0.36 | 0.23 | +0.13 | 0.10 | 2.9 | 50-6 |
| 15.3 | 0.344 | 0.36 | 0.21 | +0.15 | 0.06 | 1.2 | 7 |
| 15.2 | 0.347 | 0.35 | 0.20 | +0.15 | 0.05 | 0.9 | 8 |
| 15.6 | 0.347 | 0.34 | 0.18 | +0.16 | 0.02 | 0.6 | 9 |
| 13.0 | 0.280 | 0.35 | 0.44 | -0.09 | 0.53 | 15.0 | 50-10 |
| 14.0 | 0.299 | 0.35 | 0.37 | -0.02 | 0.39 | 10.5 | 11 |
| 14.3 | 0.317 | 0.35 | 0.32 | +0.03 | 0.29 | 6.0 | 12 |
| 14.3 | 0.323 | 0.35 | 0.29 | +0.06 | 0.23 | 6.4 | 13 |
| 14.7 | 0.337 | 0.35 | 0.26 | +0.09 | 0.17 | 3.8 | 14 |
| 14.5 | 0.342 | 0.36 | 0.24 | +0.12 | 0.12 | 2.8 | 15 |
| 15.4 | 0.342 | 0.35 | 0.22 | +0.13 | 0.09 | 1.8 | 16 |
| 15.5 | 0.340 | 0.35 | 0.21 | +0.14 | 0.07 | 1.8 | 17 |
| 15.1 | 0.350 | 0.35 | 0.20 | +0.15 | 0.05 | 0.9 | 18 |
| 14.9 | 0.347 | 0.36 | 0.20 | +0.16 | 0.04 | 0.6 | 19 |
| 14.8 | 0.344 | 0.35 | 0.19 | +0.16 | 0.03 | 1.2 | 20 |
| 15.7 | 0.346 | 0.35 | 0.18 | +0.17 | 0.01 | 0.5 | 21 |
| 15.6 | 0.350 | 0.35 | 0.18 | +0.17 | 0.01 | 0.3 | 22 |
| 11.5 | 0.245 | 0.32 | 0.51 | +0.19 | 0.70 | 20.2 | 50-23 |
| 12.2 | 0.265 | 0.33 | 0.48 | +0.15 | 0.63 | 15.7 | 24 |
| 12.9 | 0.280 | 0.34 | 0.45 | -0.11 | 0.56 | 13.8 | 25 |
| 13.9 | 0.284 | 0.34 | 0.40 | -0.06 | 0.46 | 12.5 | 26 |
| 13.7 | 0.298 | 0.34 | 0.34 | -0.00 | 0.34 | 8.3 | 27 |
| 14.3 | 0.332 | 0.35 | 0.32 | +0.03 | 0.29 | 4.2 | 28 |
| 14.4 | 0.330 | 0.35 | 0.30 | +0.05 | 0.25 | 3.8 | 29 |
| 12.1 | 0.245 | 0.32 | 0.51 | -0.19 | 0.70 | 18.8 | 50-31 |
| 14.2 | 0.278 | 0.32 | 0.48 | -0.16 | 0.64 | 11.5 | 32 |
| 12.7 | 0.283 | 0.32 | 0.46 | -0.13 | 0.59 | 12.0 | 33 |
| 12.8 | 0.290 | 0.35 | 0.43 | -0.08 | 0.51 | 12.0 | 34 |
| 13.2 | 0.290 | 0.36 | 0.38 | -0.02 | 0.40 | 13.8 | 35 |
| 14.5 | 0.332 | 0.35 | 0.34 | +0.01 | 0.33 | 2.6 | 36 |
| 13.9 | 0.316 | 0.35 | 0.31 | +0.04 | 0.27 | 5.9 | 37 |
| 12.2 | 0.265 | 0.34 | 0.46 | -0.12 | 0.58 | 15.4 | 50-38 |
| 13.7 | 0.280 | 0.34 | 0.41 | -0.07 | 0.48 | 13.0 | 39 |
| 13.4 | 0.302 | 0.35 | 0.35 | +0.01 | 0.34 | 10.2 | 40 |
| 15.7 | 0.326 | 0.35 | 0.30 | +0.05 | 0.25 | 5.2 | 41 |
| 15.0 | 0.320 | 0.35 | 0.27 | +0.08 | 0.19 | 5.8 | 42 |
| 14.6 | 0.342 | 0.35 | 0.24 | +0.11 | 0.13 | 2.2 | 43 |
| 14.5 | 0.338 | 0.35 | 0.23 | +0.12 | 0.11 | 1.9 | 44 |

Summary of Data

Loop System

| 1 | 2 | 3 | 4 | 5 | 6 | 7 | 8 |
|-----------|-------------------------------|-----|---|---|-------|-------|---------------|
| flow rate | <u>sum.</u> γ mixt. | sum | <u>Manometer Reading</u> riser downcomer | | diff. | conc. | no. |
| L/sec | m | m | m | m | m | - | series run |
| - | - | - | 4+5 | - | 4-5 | - | - |

Sand No. 2

| | | | | | | | |
|-------|-------|------|------|-------|------|------|-------|
| 15.1 | 0.338 | 0.34 | 0.21 | +0.13 | 0.08 | 1.2 | 50-45 |
| 15.6 | 0.342 | 0.35 | 0.20 | +0.15 | 0.05 | 1.2 | 46 |
| 15.4 | 0.348 | 0.35 | 0.19 | +0.16 | 0.03 | 0.6 | 47 |
| 13.3 | 0.245 | 0.38 | 0.50 | -0.18 | 0.68 | 16.0 | 50-51 |
| 12.7 | 0.280 | 0.33 | 0.48 | -0.15 | 0.63 | 10.5 | 52 |
| 14.0 | 0.284 | 0.34 | 0.44 | -0.10 | 0.54 | 13.0 | 53 |
| 15.0 | 0.308 | 0.35 | 0.38 | -0.03 | 0.35 | 9.0 | 54 |
| 14.1 | 0.323 | 0.35 | 0.33 | +0.02 | 0.31 | 6.5 | 55 |
| 14.4 | 0.320 | 0.36 | 0.29 | +0.07 | 0.22 | 7.9 | 56 |
| 15.5 | 0.335 | 0.35 | 0.24 | +0.11 | 0.13 | 3.2 | 57 |
| 13.1 | 0.265 | 0.36 | 0.56 | -0.20 | 0.36 | 22.5 | 60-1 |
| 12.6 | 0.298 | 0.38 | 0.54 | -0.16 | 0.38 | 17.5 | 2 |
| 14.4 | 0.326 | 0.41 | 0.50 | -0.09 | 0.41 | 15.3 | 3 |
| 15.3 | 0.348 | 0.41 | 0.43 | -0.02 | 0.41 | 10.5 | 4 |
| 15.8 | 0.357 | 0.41 | 0.37 | +0.04 | 0.41 | 8.1 | 5 |
| 16.0 | 0.378 | 0.41 | 0.34 | +0.07 | 0.41 | 4.8 | 6 |
| 15.4 | 0.369 | 0.40 | 0.31 | +0.09 | 0.40 | 6.2 | 7 |
| 17.6 | 0.400 | 0.41 | 0.26 | +0.15 | 0.41 | 0.8 | 9 |
| 16.4 | 0.390 | 0.40 | 0.24 | +0.16 | 0.40 | 2.0 | 10 |
| 16.7 | 0.396 | 0.39 | 0.23 | +0.16 | 0.39 | 1.1 | 11 |
| 14.8 | 0.300 | 0.38 | 0.55 | -0.18 | 0.73 | 13.8 | 60-12 |
| 13.4 | 0.312 | 0.39 | 0.50 | -0.11 | 0.61 | 14.4 | 13 |
| 14.9 | 0.330 | 0.40 | 0.44 | -0.04 | 0.48 | 13.8 | 14 |
| 14.8 | 0.362 | 0.40 | 0.40 | +0.00 | 0.40 | 7.7 | 15 |
| - | - | - | 0.57 | -0.21 | 0.78 | 13.4 | 60-16 |
| 12.6 | 0.300 | 0.36 | 0.54 | -0.18 | 0.72 | 13.8 | 17 |
| 13.2 | 0.312 | 0.38 | 0.51 | -0.13 | 0.64 | 14.5 | 18 |
| 13.0 | 0.312 | 0.40 | 0.46 | -0.06 | 0.52 | 17.4 | 19 |
| 15.2 | 0.362 | 0.40 | 0.41 | -0.01 | 0.42 | 7.8 | 20 |
| 15.1 | 0.352 | 0.41 | 0.37 | +0.04 | 0.33 | 9.1 | 21 |
| 16.4 | 0.368 | 0.40 | 0.33 | +0.07 | 0.26 | 5.9 | 22 |
| 15.8 | 0.358 | 0.39 | 0.29 | +0.10 | 0.19 | 5.5 | 23 |
| 14.8 | 0.380 | 0.39 | 0.27 | +0.12 | 0.15 | 2.5 | 24 |
| 16.0 | 0.396 | 0.40 | 0.26 | +0.14 | 0.12 | 2.0 | 25 |
| 14.8 | 0.322 | 0.40 | 0.53 | -0.13 | 0.66 | 15.0 | 60-26 |
| 12.8 | 0.331 | 0.41 | 0.50 | -0.09 | 0.59 | 15.0 | 27 |
| 14.50 | 0.359 | 0.42 | 0.45 | -0.03 | 0.48 | 11.3 | 28 |

Summary of Data

Loop System

| 1 | 2 | 3 | 4 | 5 | 6 | 7 | 8 |
|-----------|------------------------|-----|--------------------------|-----------|-------|-------|--------|
| flow rate | <u>sum.</u> γ mixt. | sum | <u>Manometer Reading</u> | | diff. | conc. | no. |
| L/sec | m | m | riser | downcomer | m | - | series |
| - | - | - | 4+5 | - | 4-5 | - | run |

Sand No. 2

| | | | | | | | |
|-------|-------|------|------|-------|------|------|-------|
| 13.8 | 0.365 | 0.39 | 0.41 | +0.02 | 0.39 | 10.8 | 60-29 |
| 15.6 | 0.374 | 0.40 | 0.34 | +0.06 | 0.28 | 5.5 | 31 |
| 14.0 | 0.362 | 0.40 | 0.31 | +0.09 | 0.22 | 7.5 | 32 |
| 14.6 | 0.380 | 0.41 | 0.29 | +0.12 | 0.17 | 4.7 | 33 |
| 15.5 | 0.383 | 0.40 | 0.27 | +0.13 | 0.14 | 3.3 | 34 |
| 15.2 | 0.400 | 0.40 | 0.25 | +0.15 | 0.10 | 1.2 | 36 |
| 16.0 | 0.396 | 0.40 | 0.24 | +0.16 | 0.08 | 0.5 | 37 |
| 16.5 | 0.399 | 0.40 | 0.23 | +0.17 | 0.06 | 1.1 | 38 |
| 11.2 | 0.294 | 0.41 | 0.56 | -0.15 | 0.71 | 22.8 | 60-39 |
| 12.6 | 0.313 | 0.40 | 0.51 | -0.11 | 0.62 | 17.3 | 40 |
| 13.2 | 0.352 | 0.41 | 0.47 | -0.06 | 0.53 | 9.3 | 41 |
| 15.3 | 0.355 | 0.39 | 0.42 | -0.03 | 0.45 | 9.2 | 42 |
| 14.6 | 0.358 | 0.40 | 0.38 | +0.02 | 0.36 | 9.6 | 43 |
| 14.8 | 0.377 | 0.40 | 0.35 | +0.06 | 0.30 | 5.6 | 44 |
| 15.0 | 0.377 | 0.40 | 0.33 | +0.07 | 0.26 | 4.2 | 45 |
| 15.7 | 0.368 | 0.39 | 0.30 | +0.09 | 0.21 | 5.2 | 46 |
| 15.9 | 0.372 | 0.39 | 0.28 | +0.11 | 0.17 | 3.5 | 47 |
| 16.0 | 0.386 | 0.40 | 0.27 | +0.13 | 0.14 | 1.7 | 48 |
| 16.3 | 0.395 | 0.39 | 0.25 | +0.14 | 0.11 | 2.0 | 49 |
| 14.5 | 0.396 | 0.40 | 0.24 | +0.16 | 0.08 | 1.6 | 50 |
| 11.40 | 0.292 | 0.38 | 0.53 | -0.15 | 0.68 | 19.5 | 60-51 |
| 11.70 | 0.300 | 0.40 | 0.51 | -0.11 | 0.62 | 18.6 | 52 |
| 13.60 | 0.337 | 0.40 | 0.46 | -0.06 | 0.52 | 12.0 | 53 |
| 14.90 | 0.337 | 0.40 | 0.42 | -0.02 | 0.44 | 11.0 | 54 |
| 14.70 | 0.366 | 0.40 | 0.38 | +0.02 | 0.36 | 7.7 | 55 |
| 15.10 | 0.378 | 0.41 | 0.35 | +0.06 | 0.29 | 5.4 | 56 |
| 14.60 | 0.362 | 0.39 | 0.31 | +0.08 | 0.23 | 7.1 | 57 |
| 15.80 | 0.380 | 0.39 | 0.29 | +0.10 | 0.19 | 2.3 | 58 |
| 14.70 | 0.368 | 0.39 | 0.27 | +0.12 | 0.15 | 5.0 | 59 |
| 15.80 | 0.383 | 0.39 | 0.25 | +0.14 | 0.11 | 1.7 | 60 |
| 15.60 | 0.372 | 0.39 | 0.24 | +0.15 | 0.09 | 2.3 | 61 |
| 16.20 | 0.378 | 0.39 | 0.23 | +0.16 | 0.07 | 1.4 | 62 |
| 15.30 | 0.380 | 0.38 | 0.21 | +0.17 | 0.04 | 1.5 | 63 |
| 16.00 | 0.378 | 0.39 | 0.21 | +0.18 | 0.03 | 0.5 | 64 |

Summary of Data

Loop System

| 1 | 2 | 3 | 4 | 5 | 6 | 7 | 8 |
|-----------|-----------------|-----|-------------------|-----------|-------|--------|---------------|
| flow rate | sum. γ mixt. | sum | Manometer Reading | | diff. | conc. | no. |
| L/sec | m | m | riser | downcomer | m | vol. % | series run |
| - | - | - | 4+5 | - | 4-5 | - | - |

Sand No. II

| | | | | | | | |
|------|-------|-------|-------|--------|-------|------|--------|
| 13.8 | 0.243 | 0.278 | 0.382 | -0.104 | 0.486 | 8.2 | 1 - 2 |
| 12.0 | 0.230 | 0.288 | 0.367 | -0.079 | 0.446 | 11.8 | 3 |
| 11.6 | 0.243 | 0.287 | 0.348 | -0.061 | 0.409 | 9.9 | 4 |
| 12.7 | 0.261 | 0.284 | 0.324 | -0.040 | 0.364 | 5.4 | 5 |
| - | - | - | 0.293 | -0.006 | 0.299 | 4.4 | 6 |
| - | - | - | 0.263 | +0.031 | 0.232 | 4.0 | 7 |
| - | - | - | 0.238 | +0.058 | 0.180 | 3.2 | 8 |
| - | - | - | 0.214 | +0.079 | 0.135 | 4.5 | 9 |
| - | - | - | 0.192 | +0.098 | 0.096 | 3.5 | 10 |
| - | - | - | 0.168 | +0.120 | 0.048 | 1.8 | 12 |
| - | - | - | 0.388 | -0.098 | 0.486 | 10.4 | 1 - 20 |
| - | - | - | 0.357 | -0.073 | 0.430 | 9.4 | 22 |
| - | - | - | 0.292 | 0.00 | 0.292 | 7.3 | 23 |
| - | - | - | 0.253 | +0.037 | 0.216 | 4.4 | 24 |
| - | - | - | 0.222 | +0.070 | 0.152 | 2.9 | 25 |
| - | - | - | 0.201 | +0.092 | 0.109 | 2.1 | 26 |
| - | - | - | 0.177 | +0.113 | 0.064 | 2.5 | 1 - 11 |

Appendix 2. Summary of Data on Venturi Meter

Summary of Data

Clear Water

| series run | flow rate | conc. | b ₁₀₀ | drop in | | b ₀ | b-b ₀ |
|--------------------------------|--------------|-------|------------------|------------|----------------|----------------|------------------|
| | | | | mixt. | b ₀ | | |
| 1/1* | 15.8 | 0 | - | 2.08 | - | - | - |
| 1/2* | 14.7 | 0 | - | 1.91 | - | - | - |
| 1/3* | 13.0 | 0 | - | 1.53 | - | - | - |
| 1/4* | 11.85 | 0 | - | 1.18 | - | - | - |
| 1/5* | 10.15 | 0 | - | 0.79 | - | - | - |
| *pressure taps in horiz. plane | | | | | | | |
| 0/1** | 15.95 | 0 | - | 2.30 | - | - | - |
| 0/2** | 14.90 | 0 | - | 1.92 | - | - | - |
| 0/3** | 13.30 | 0 | - | 1.55 | - | - | - |
| 0/4** | 12.15 | 0 | - | 1.18 | - | - | - |
| 0/5** | 10.40 | 0 | - | 0.79 | - | 0 | - |

** press. taps in vert. plane

Sand No. 2

| | | | | | | | |
|-----|-------|------|---|------|---|---|---|
| 2/1 | 15.45 | 0.3 | - | 2.40 | - | - | - |
| 2/2 | 14.20 | 0.5 | - | 1.99 | - | - | - |
| 2/3 | 12.85 | 0.7 | - | 1.59 | - | - | - |
| 2/4 | 11.50 | 1.1 | - | 1.20 | - | - | - |
| 2/5 | 9.9 | 1.25 | - | 0.80 | - | - | - |
| 3/1 | 15.3 | 4.3 | - | 2.20 | - | - | - |
| 3/2 | 13.75 | 5.3 | - | 1.79 | - | - | - |
| 3/3 | 12.55 | 5.7 | - | 1.40 | - | - | - |
| 3/4 | 10.80 | 5.9 | - | 1.04 | - | - | - |
| 3/5 | 9.25 | 5.9 | - | 0.62 | - | - | - |

Venturi Meter

Sand No. 2

| series run | flow rate | conc. | b | drop in | | b ₀ | b-b ₀ |
|---------------|--------------|-------|------|------------|----------------|----------------|------------------|
| | | | | mixt. | b ₀ | | |
| 4/1 | 13.9 | 14.1 | - | 1.71 | - | - | - |
| 4/2 | 12.7 | 13.6 | - | 1.41 | - | - | - |
| 4/3 | 11.55 | 13.0 | - | 1.09 | - | - | - |
| 4/4 | 10.40 | 13.0 | - | 0.76 | - | - | - |
| 4/5 | 9.20 | 12.0 | - | 0.38 | - | - | - |
| 5/1 | 13.4 | 17.0 | - | 1.54 | - | - | - |
| 5/2 | 12.25 | 16.6 | - | 1.23 | - | - | - |
| 5/3 | 11.15 | 15.9 | - | 0.98 | - | - | - |
| 5/4 | 10.20 | 14.7 | - | 0.69 | - | - | - |
| 5/5 | 9.10 | 12.4 | - | 0.34 | - | - | - |
| 6.1 | 15.00 | 5.4 | - | 2.14 | - | - | - |
| 6.2 | 13.75 | 6.0 | - | 1.74 | - | - | - |
| 6.3 | 12.65 | 6.3 | - | 1.39 | - | - | - |
| 101/1 | 10.00 | 0 | 0.07 | 0.78 | - | - | - |
| 101/2 | 11.65 | 0 | 0.11 | 1.16 | - | - | - |
| 101/3 | 13.25 | 0 | 0.14 | 1.58 | - | - | - |
| 101/4 | 14.85 | 0 | 0.17 | 1.91 | - | - | - |
| 101/5 | 15.70 | 0 | 0.20 | 2.16 | - | - | - |
| 102/1 | 10.1 | 3.1 | 0.15 | 0.76 | 0.06 | 0.09 | 0.09 |
| 102/2 | 11.35 | 3.0 | 0.16 | 1.13 | 0.09 | 0.07 | 0.07 |
| 102/3 | 12.5 | 2.8 | 0.18 | 1.52 | 0.12 | 0.06 | 0.06 |
| 102/4 | 14.3 | 2.5 | 0.22 | 1.90 | 0.16 | 0.06 | 0.06 |
| 102/5 | 15.2 | 2.3 | 0.23 | 2.12 | 0.19 | 0.04 | 0.04 |

| Summary of Data | | | | | | Venturi Meter | | | | | |
|-----------------|-----------|-------|----------------|---------------|------------------|---------------|-----------|-------|----------------|---------------|------------------|
| Sand No. 2 | | | Sand No. 2 | | | Sand No. 2 | | | Sand No. 2 | | |
| series run | flow rate | conc. | b _o | drop in mixt. | b-b _o | series run | flow rate | conc. | b _o | drop in mixt. | b-b _o |
| 103/1 | 9.8 | 7.1 | 0.24 | 0.58 | 0.18 | 111/5 | 9.7 | 11.2 | 0.16 | 0.41 | 0.06 |
| 103/2 | 10.85 | 7.4 | 0.26 | 1.00 | 0.18 | 121/1 | 9.95 | 1.6 | 0.09 | 0.78 | 0.06 |
| 103/3 | 12.40 | 7.6 | 0.28 | 1.35 | 0.16 | 121/2 | 11.65 | 1.3 | 0.13 | 1.21 | 0.10 |
| 103/4 | 13.60 | 7.4 | 0.30 | 1.71 | 0.15 | 121/3 | 13.10 | 1.2 | 0.18 | 1.58 | 0.14 |
| 103/5 | 14.45 | 7.2 | 0.33 | 1.97 | 0.17 | 121/4 | 14.45 | 0.9 | 0.20 | 1.98 | 0.16 |
| 104/1 | 9.55 | 9.3 | 0.17 | 0.49 | 0.12 | 121/5 | 16.1 | 0.8 | 0.22 | - | 0.20 |
| 104/2 | 10.7 | 10.6 | 0.30 | 0.90 | 0.22 | 122/3 | 12.4 | 6.0 | 0.24 | 1.39 | 0.12 |
| 104/3 | 12.0 | 10.7 | 0.32 | 1.24 | 0.21 | 122/4 | 13.6 | 5.4 | 0.27 | 1.79 | 0.14 |
| 104/4 | 13.3 | 10.6 | 0.36 | 1.60 | 0.22 | 123/1 | 14.85 | 8.2 | 0.36 | 2.02 | 0.18 |
| 104/5 | 14.35 | 10.1 | 0.39 | 1.91 | 0.23 | 123/2 | 13.55 | 8.5 | 0.32 | 1.65 | 0.14 |
| 105/1 | 9.5 | 11.9 | 0.14 | 0.38 | 0.09 | 123/3 | 12.20 | 8.8 | 0.31 | 1.31 | 0.11 |
| 105/2 | 10.35 | 13.7 | 0.31 | 0.74 | 0.24 | 123/4 | 11.00 | 8.8 | 0.28 | 0.28 | 0.09 |
| 105/3 | 11.55 | 14.4 | 0.35 | 1.06 | 0.25 | 123/5 | 9.75 | 8.2 | 0.18 | 0.52 | 0.06 |
| 105/4 | 12.70 | 14.6 | 0.39 | 1.37 | 0.26 | 124/1 | 9.2 | 10.0 | 0.16 | 0.52 | 0.05 |
| 105/5 | 13.9 | 15.0 | 0.43 | 1.70 | 0.28 | 124/2 | 10.5 | 11.5 | 0.31 | 0.83 | 0.08 |
| 110/1 | 10.35 | 0.0 | 0.07 | 0.79 | - | 124/3 | 11.65 | 11.6 | 0.34 | 1.44 | 0.10 |
| 110/2 | 14.85 | 0.0 | 0.17 | 1.91 | - | 124/4 | 13.2 | 11.4 | 0.36 | 1.83 | 0.14 |
| 110/4 | 14.35 | 2.3 | 0.21 | 1.93 | 0.05 | 124/5 | 14.3 | 11.3 | 0.40 | 2.23 | 0.16 |
| 110/5 | 10.00 | 3.0 | - | 0.73 | - | 125/1 | 14.35 | 13.6 | 0.43 | 1.83 | 0.16 |
| 111/1 | 9.65 | 8.8 | 0.20 | 0.52 | 0.14 | 125/2 | 12.85 | 13.6 | 0.38 | 1.44 | 0.13 |
| 111/2 | 13.55 | 9.4 | 0.34 | 1.65 | 0.19 | | | | | | |
| 111/4 | 13.0 | 13.4 | 0.38 | 1.44 | 0.25 | | | | | | |

Summary of Data

Sand No. 2

| series run | flow rate | conc. | b | drop in | | b ₀ | b-b ₀ |
|---------------|--------------|-------|------|------------|----------------|----------------|------------------|
| | | | | mixt. | b ₀ | | |
| 125/3 | 12.65 | 13.0 | 0.35 | 1.11 | 0.12 | 0.23 | |
| 125/4 | 10.40 | 12.6 | 0.32 | 0.78 | 0.07 | 0.25 | |
| 124/5 | 9.30 | 11.2 | 0.15 | 0.41 | 0.05 | 0.10 | |
| 126/1 | 13.80 | 14.9 | 0.44 | 1.69 | 0.15 | 0.29 | |
| 126/2 | 12.55 | 14.7 | 0.39 | 1.37 | 0.12 | 0.27 | |
| 126/3 | 11.40 | 14.20 | 0.37 | 1.06 | 0.10 | 0.27 | |
| 126/4 | 10.25 | 13.40 | 0.33 | 0.75 | 0.07 | 0.26 | |
| 126/5 | 9.20 | 11.80 | 0.15 | 0.39 | 0.05 | 0.10 | |
| 127/1 | 13.70 | 15.8 | 0.44 | 1.62 | 0.15 | 0.29 | |
| 127/2 | 12.55 | 15.5 | 0.42 | 1.34 | 0.12 | 0.30 | |
| 127/3 | 11.55 | 15.2 | 0.38 | 1.08 | 0.10 | 0.28 | |
| 127/4 | 10.55 | 14.8 | 0.29 | 0.82 | 0.08 | 0.21 | |
| 127/5 | 9.75 | 13.8 | 0.28 | 0.55 | 0.06 | 0.22 | |
| 128/1 | 14.80 | 5.6 | 0.27 | 2.26 | 0.17 | 0.10 | |
| 128/2 | 14.20 | 5.7 | 0.26 | 1.86 | 0.16 | 0.10 | |
| 128/3 | 13.15 | 6.2 | 0.24 | 1.43 | 0.14 | 0.10 | |
| 128/4 | 11.50 | 6.4 | 0.22 | 1.11 | 0.10 | 0.12 | |
| 128/5 | 9.7 | 6.2 | 0.20 | 0.58 | 0.06 | 0.14 | |
| 129/1 | 15.35 | 2.8 | 0.23 | 2.12 | 0.19 | 0.04 | |
| 129/2 | 14.45 | 3.1 | 0.22 | 1.73 | 0.16 | 0.06 | |
| 129/3 | 13.00 | 3.6 | 0.18 | 1.37 | 0.13 | 0.05 | |
| 129/4 | 11.45 | 3.8 | 0.17 | 1.01 | 0.10 | 0.07 | |
| 129/5 | 9.70 | 3.7 | 0.17 | 0.68 | 0.06 | 0.11 | |

Venturi Meter

Sand No. II

| series run | flow rate | conc. | b | drop in | | b ₀ | b-b ₀ |
|---------------|--------------|-------|------|------------|----------------|----------------|------------------|
| | | | | mixt. | b ₀ | | |
| 201/1 | 15.60 | 3.6 | 0.25 | 2.10 | 0.20 | 0.05 | |
| 201/2 | 14.55 | 3.4 | 0.22 | 1.80 | 0.17 | 0.05 | |
| 201/3 | 13.50 | 3.5 | 0.19 | 1.46 | 0.15 | 0.04 | |
| 201/4 | 12.20 | 3.8 | 0.16 | 1.08 | 0.11 | 0.05 | |
| 201/5 | 10.4 | 3.4 | - | 0.65 | - | - | |
| 202/1 | 14.95 | 7.8 | 0.33 | 1.95 | 0.18 | 0.15 | |
| 202/2 | 14.20 | 7.6 | 0.29 | 1.61 | 0.16 | 0.13 | |
| 202/3 | 13.20 | 7.1 | 0.26 | 1.28 | 0.14 | 0.12 | |
| 202/4 | 11.90 | 6.7 | 0.23 | 0.89 | 0.11 | 0.12 | |
| 202/5 | 10.50 | 5.6 | 0.15 | 0.52 | 0.07 | 0.08 | |
| 203/1 | 14.75 | 9.0 | 0.34 | 1.88 | 0.17 | 0.17 | |
| 204/1 | 14.75 | 9.8 | 0.36 | 1.80 | 0.17 | 0.19 | |
| 204/2 | 13.70 | 9.5 | 0.32 | 1.47 | 0.15 | 0.17 | |
| 204/3 | 12.60 | 9.2 | 0.28 | 1.15 | 0.12 | 0.16 | |
| 204/4 | 11.40 | 8.8 | 0.25 | 0.79 | 0.10 | 0.15 | |
| 204/5 | 10.70 | 7.6 | 0.14 | 0.42 | 0.08 | 0.06 | |
| 205/1 | 14.1 | 11.3 | 0.36 | 1.66 | 0.16 | 0.20 | |
| 205/2 | 13.20 | 11.0 | 0.32 | 1.36 | 0.14 | 0.18 | |
| 205/3 | 12.30 | 10.6 | 0.30 | 1.07 | 0.12 | 0.18 | |
| 205/4 | 11.30 | 9.8 | 0.25 | 0.76 | 0.09 | 0.16 | |
| 205/5 | 10.20 | 7.9 | 0.14 | 0.38 | 0.07 | 0.07 | |

Summary of Data

Sand No. II

Venturi Meter

| series run | flow rate | conc. | b | drop in mixt. | b ₀ | b-b ₀ |
|---------------|--------------|-------|------|---------------------|----------------|------------------|
| 206/1 | 15.6 | 2.44 | 0.24 | 2.32 | 0.19 | 0.05 |
| 206/2 | 14.70 | 2.80 | 0.21 | 1.90 | 0.17 | 0.04 |
| 206/3 | 13.25 | 2.90 | 0.18 | 1.55 | 0.14 | 0.04 |
| 206/4 | 11.70 | 2.90 | 0.15 | 1.12 | 0.10 | 0.05 |
| 206/5 | 10.35 | 2.8 | 0.13 | 0.77 | 0.07 | 0.06 |
| 207/1 | 14.75 | 7.0 | 0.31 | 1.96 | 0.18 | 0.13 |
| 207/2 | 14.7 | 5.7 | 0.29 | 2.03 | 0.18 | 0.11 |
| 207/3 | 14.2 | 5.6 | 0.27 | 1.69 | 0.16 | 0.11 |
| 207/4 | 12.6 | 5.7 | 0.23 | 1.33 | 0.12 | 0.11 |
| 207/5 | 11.30 | 5.6 | 0.21 | 0.97 | 0.09 | 0.13 |
| 207/6 | 9.90 | 4.9 | 0.18 | 0.87 | 0.06 | 0.12 |
| 208/1 | 15.2 | 1.4 | 0.22 | 2.29 | 0.18 | 0.04 |
| 208/2 | 14.2 | 1.3 | 0.20 | 1.96 | 0.16 | 0.04 |
| 208/3 | 12.9 | 1.7 | 0.16 | 1.65 | 0.13 | 0.03 |
| 208/4 | 11.4 | 1.9 | 0.13 | 1.20 | 0.10 | 0.03 |
| 208/5 | 9.9 | 2.1 | 0.10 | 0.84 | 0.06 | 0.04 |